Responses to comments of "Susceptibility of Marine Warm Clouds to Aerosols in Different Monsoon Periods over the South China Sea" (Manuscript ID: egusphere-2025-5935) to *Atmospheric Chemistry and Physics*.

Yan Liu, Hailing Jia, Yong Han*

We are grateful to the reviewers for their thoughtful and constructive comments, which are very helpful for improving the quality of this manuscript. We have thoroughly revised the manuscript to address all comments with the point-by-point responses. We hope that the revised version can obtain favorable approval and meet the journal requirements. The referee's comments are reproduced (*black*, *italic*) along with our replies (blue) and changes made to the text (red) in the revised manuscript. All the authors have read the revised manuscript and agreed with the submission in its revised form.

Responses to Reviewer #1

This manuscript examines the susceptibility of marine warm clouds to aerosol loading over the South China Sea (SCS) under contrasting monsoon regimes, using CERES–MODIS cloud retrievals and MERRA-2 aerosol reanalysis. The monsoon period is classified into three phases (SWMW, NEMW, NEMD), and the study investigates how humidity and lower-tropospheric stability modulate ACI. The topic is relevant given the limited observational constraints on ACI over the SCS, and the scientific question of how monsoon-driven environmental contrasts regulate ACI is well motivated and worth pursuing.

While the manuscript is designed in a self-consistent and logical way, I have noticed several concerns, some of which are fundamental, that inevitably compromise the scientific robustness of the results and conclusions. These include the Nd retrieval methodology, the ACI metric definition, the choice of aerosol proxy, and the absence of cloud-regime separation, each of which introduces systematic biases or confounds that propagate into the core analysis. I am therefore unfortunately unable to recommend publication in its current form, though I would encourage resubmission after carefully considering the main concerns listed below. I recognize that some may be challenging to address in full, but I would appreciate at least the consideration of adopting more robust satellite datasets and a rigorous discussion of the potential uncertainties and limitations.

Response:

We sincerely thank the reviewer for the constructive and insightful comments. We fully acknowledge the concerns raised regarding the potential biases and uncertainties associated with our original data processing and methodological framework, and we greatly appreciate the reviewer's valuable suggestions for improving the scientific robustness of this study. In response, we have implemented substantial revisions to address these concerns. Specifically, we recognized the limitations of retrieving Nd at the 1° × 1° resolution in our original analysis and have replaced the self-retrieved Nd with the more robust satellite-derived product from Grosvenor et al. (2018). We have also revised the definition of the ACI metric, clarified the selection of the aerosol proxy, and further classified cloud regimes. We have provided point-by-point responses to your valuable suggestions, aiming to address these issues and enhance the quality of the manuscript.

Comments:

Comment #1:

ACI_{Nd} definition:

The definition of ACI_{Nd} in Eq. (2) appears to be inconsistent with the standard formulation used by the community. As originally defined by Feingold et al. (2001) and subsequently adopted by McComiskey et al. (2009) and McComiskey and Feingold (2012), the Nd susceptibility (ACI_{Nd}) is given by:

$$\mathrm{ACI}_{Nd} = d\ln N_d / d\ln \alpha$$

where α is an aerosol proxy (e.g., AOD, AI, or NCCN). The factor of 1/3 actually relates the two ACI metrics to each other through the Twomey relationship: at constant liquid water path, Nd $\propto$ res, so that $ACI_r \approx (1/3) \cdot ACI_{Nd}$. Thus this factor of 1/3 is a theoretical conversion between the two metrics, not a component within the definition of ACI_{Nd} itself.

However, Eq. (2) in the manuscript defines ACI_{Nd} = d ln Nd / 3 d ln NCCN, which places the factor of 3 in the denominator of the ACI_{Nd} expression. This formulation would yield ACI_{Nd} values that are systematically one-third of those obtained using the

standard definition, thereby underestimating the Nd susceptibility to aerosols. Please clarify whether this is a typo in the equation (with the actual calculations performed correctly using d ln Nd / d ln NCCN), or whether the factor of 1/3 was indeed applied in the computation. If the latter is the case, all reported ACI_{Nd} values would need to be recalculated, and any quantitative comparison with other studies that use the standard definition would be invalid.

Response:

We sincerely thank the reviewer for pointing out the issue regarding the definition of ACI_{Nd}. We acknowledge that the definition used in the original manuscript was inconsistent with the standard formulation. We confirm that the factor of 1/3 was indeed applied in the original calculations, which led to an underestimation of the reported ACI_{Nd} values. we have corrected Eq. (2) to adopt the standard definition of ACI_{Nd} and have recalculated all ACI_{Nd} accordingly throughout the manuscript. Although the absolute magnitudes have been adjusted, the recalculated results remain qualitatively consistent with those presented in the original manuscript, and all key scientific conclusions are unchanged. All related results, figures, and corresponding discussions have been updated in the revised version to ensure consistency with the conventional definition used in the literature.

Changes in Manuscript:

[Page 4, Line 74-78 (in the "Track Changes" version)]

$$\mathrm{ACI}_r = -d\ln r / d\ln \alpha \qquad (1)$$

$$\mathrm{ACI}_{Nd} = d\ln N_d / d\ln \alpha \qquad (2)$$

where r and N_d denote the cloud effective radius and droplet number concentration, respectively, and α is an aerosol proxy (e.g., AOD, AI, or NCCN). In this study, AI is employed as the aerosol proxy in the calculation of ACI.

[Page 25-26, Line 449-451 (in the "Track Changes" version)]

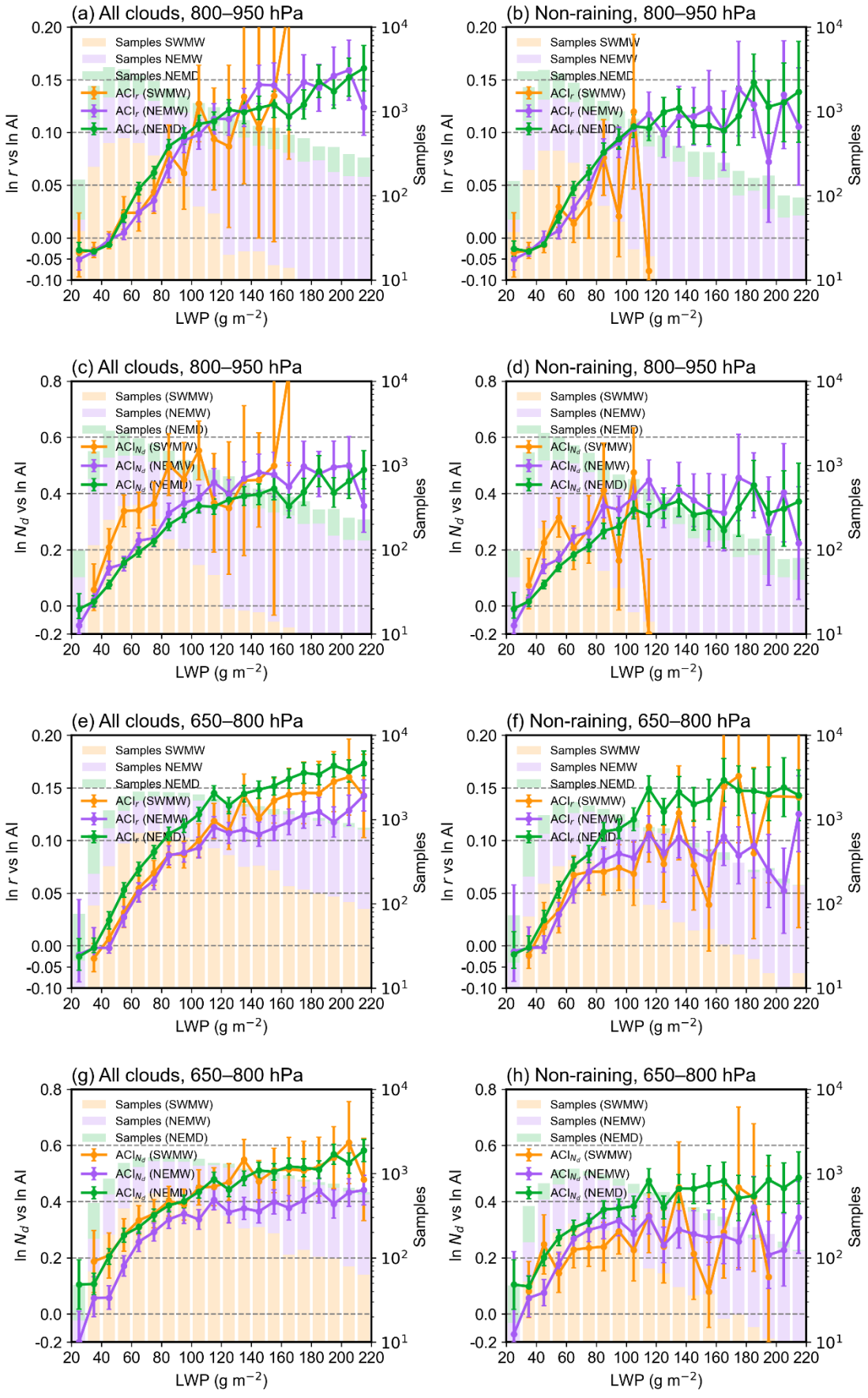

Figure 8: Linear regression slopes of ln CER versus ln AI and ln N_d versus ln AI for shallow stratocumulus clouds (CTP = 800–950 hPa; a–d) and deeper cumulus clouds (CTP = 650–800 hPa; e–h) during the three periods. The first and second columns represent all cloud and non-raining cloud conditions, respectively. Green, purple, and yellow lines represent the southwest monsoon, northeast monsoon wet period, and northeast monsoon dry period, respectively. Error bars denote the 95 % confidence intervals of the linear regressions. Colored bars, consistent with the line colors, indicate the total number of samples within each LWP bin for the corresponding periods.

[Page 28-29, Line 499-510 (in the "Track Changes" version)]

In addition to the radius-based ACI_r, we further examined the droplet-number susceptibility (ACI_{Nd}) separately for shallow stratocumulus (Fig. 8c–d) and deeper cumulus clouds (Fig. 8g–h). Consistent with the ACI_r results, ACI_{Nd} for shallow stratocumulus remains broadly comparable across the three monsoon periods, with no significant differences. Deeper cumulus clouds exhibit clear period-to-period variations, with the strongest signals occurring during the NEMD period, while comparatively weaker values are observed during the SWMW and NEMW periods. Such consistency highlights that the observed period-to-period differences in ACI are governed by systematic changes in the underlying meteorological environment rather than by the choice of ACI metric. Motivated by this consistency, Section 3.5 investigates how variations in moisture and LTS regulate the evolution of deeper cumulus clouds ACI across the three periods.

[Page 30-31, Line 536-54 (in the "Track Changes" version)]

To provide an integrated view of how the ACI of deeper cumulus clouds co-varies with the thermodynamic and moisture background across the three periods, Fig. 9 shows the ACI_{Nd} together with the corresponding q and LST. Both ACI_{Nd} and the key environmental regulators display a coherent evolution across the three periods. From the SWMW to the NEMW and NEMD, ACI_{Nd} intensify steadily, in parallel with declining moisture and increasing LTS. Quantitatively, The ACI_{Nd} increases progressively from 0.250 ± 0.027 (95% confidence interval, 95% CI) during the SWMW period to 0.286 ± 0.016 during NEMW and further to 0.399 ± 0.029 during NEMD. Meanwhile, q decreases from 12.111 ± 0.540 g kg^{-1} during SWMW to 11.072 ± 0.931 g kg^{-1} during NEMW and 9.540 ± 1.120 g kg^{-1} during NEMD, while the LTS

increases from 13.341 ± 0.358 K to 14.565 ± 0.875 K and 15.343 ± 0.977 K, respectively. (All q and LTS uncertainties represent one standard deviation, std.) These co-varying changes indicate that both q and LTS may regulate the strengthening of ACI across the three periods over the SCS. In the following subsections, we separately examine the roles of q (Section 3.5.1) and LTS (Section 3.5.2) in regulating ACI.

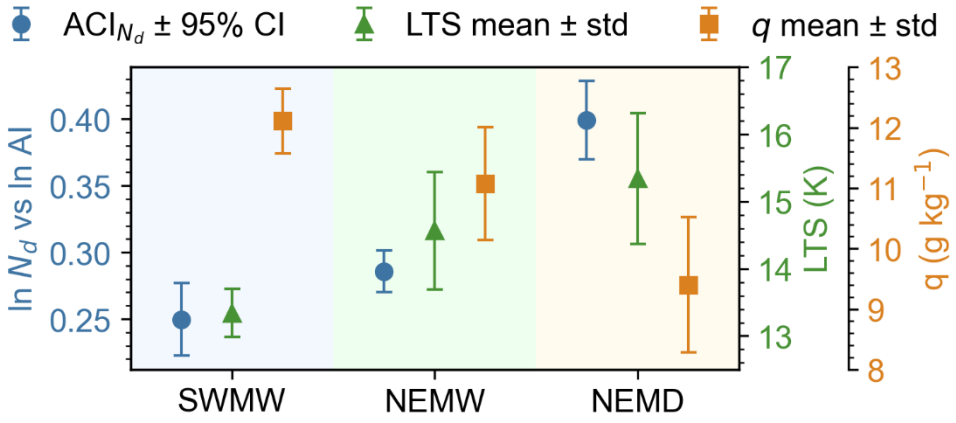

Figure 9: ACI$_{Nd}$, specific humidity (q), and lower-tropospheric stability (LTS) for the three periods over the South China Sea. The 95% confidence interval (CI) represents the uncertainty derived from the Student's t test, whereas std denotes the one standard deviation.

[Page 32-33, Line 570-581 (in the "Track Changes" version)]

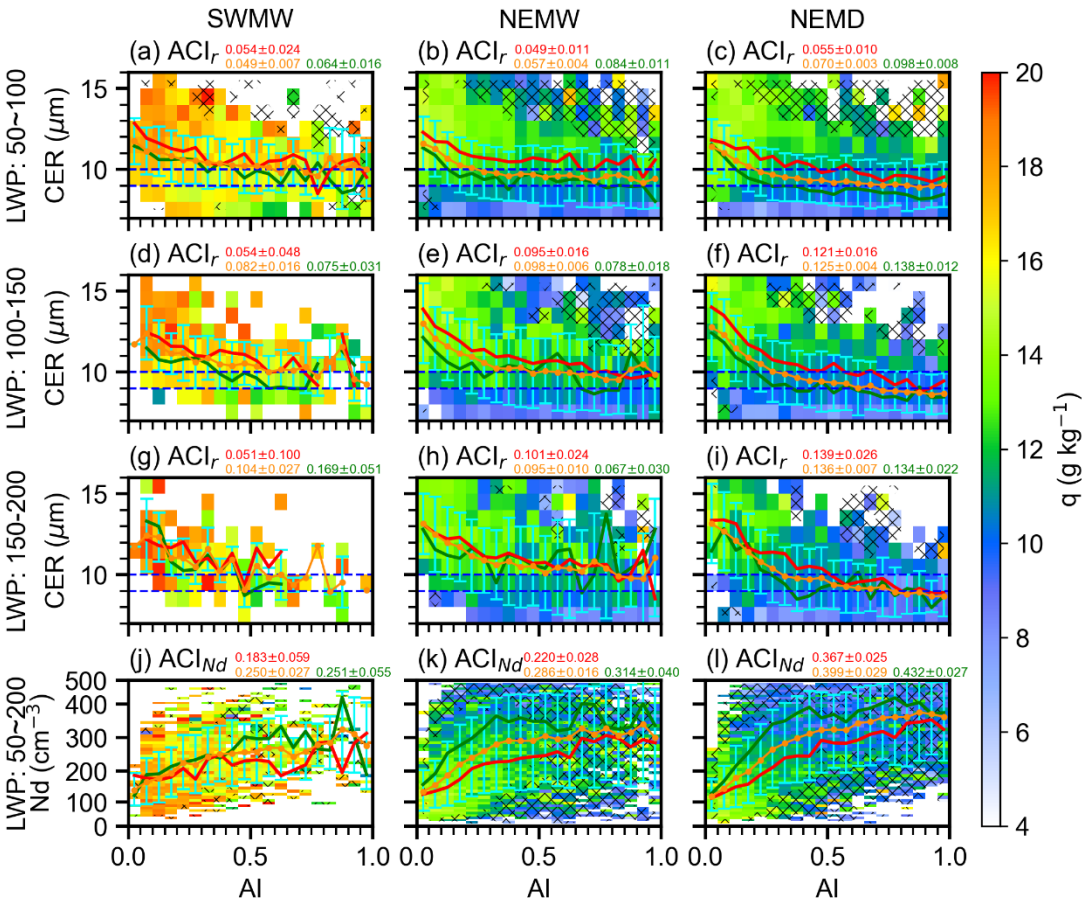

Figure 10: Influence of water vapor on ACI in deeper cumulus clouds (CTP: 650-800 hPa) across the three periods. Rows 1–3 show mean specific humidity in CER–AI bins for LWP ranges of 50–100, 100–150, and 150–200 g m^{-2}, respectively; row 4 shows mean specific humidity in N_d-AI bins for LWP 50–200 g m^{-2}. Columns correspond to the southwest monsoon, northeast monsoon wet period, and northeast monsoon dry period. Yellow dashed, red, and green lines denote the mean CER (rows 1–3) or N_d (row 4) in each AI bin for all samples, for moist conditions (specific humidity > 75th percentile), and for dry conditions (specific humidity < 25th percentile), respectively. Error bars indicate the standard deviation of CER (rows 1–3) or Nd (row 4) within each AI bin. Yellow numbers indicate ACI ± 95% uncertainty estimates (according to a Student's t test) for all samples, whereas red and green numbers indicate the corresponding estimates under moist and dry conditions, respectively.

[Page 36-37, Line 639-644 (in the "Track Changes" version)]

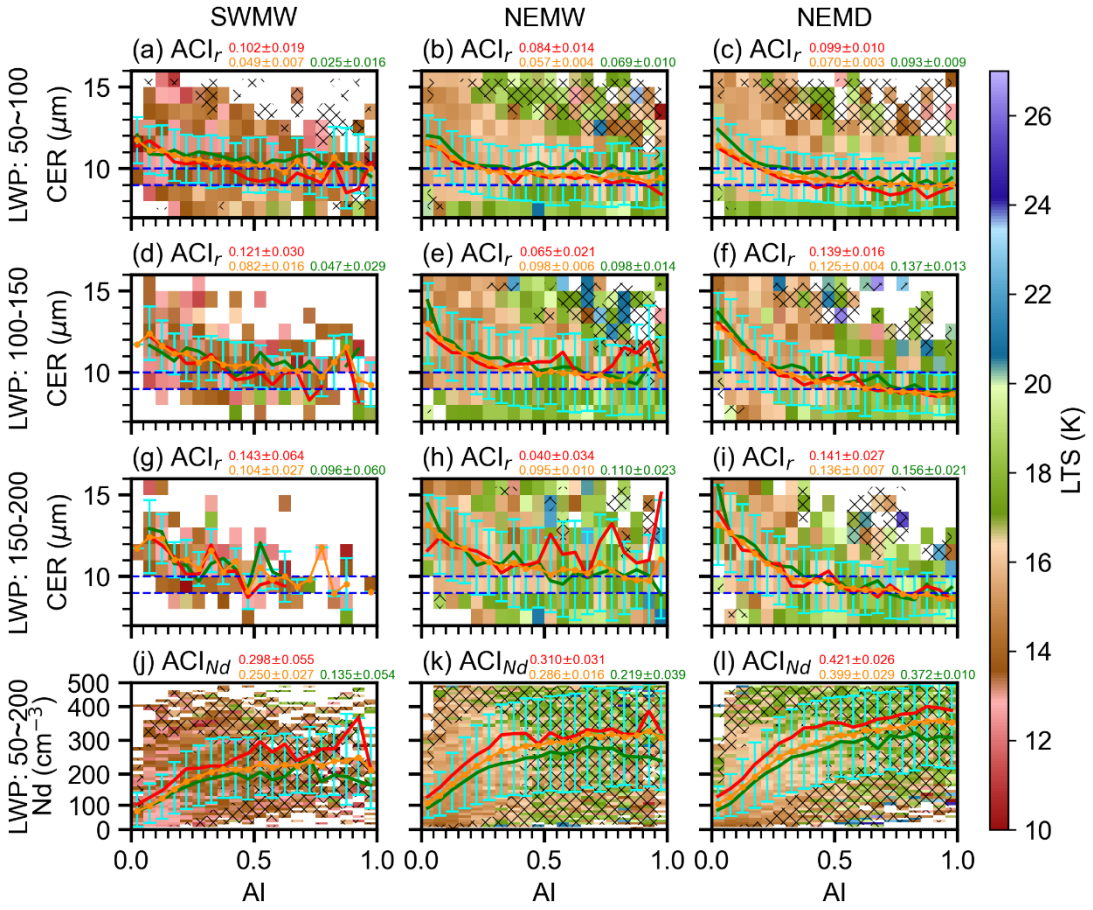

Figure 11: Same as Fig. 10, but for lower tropospheric stability. Stable and unstable conditions correspond to the upper (> 75th percentile) and lower (< 25th percentile) quartiles of LTS, respectively. Yellow numbers indicate ACI ± 95% uncertainty estimates (according to a Student's t test) for all samples, whereas red and green numbers indicate the corresponding estimates under stable and unstable conditions, respectively.

Comment #2:

Study period and Aqua orbit drift:

The entire study period (January 2022 to February 2023) coincides with Aqua's free-drift phase. Aqua completed its last orbit-maintenance maneuver in December 2021 and its mean local equatorial crossing time drifted progressively from the nominal 1:30 PM, exceeding the 1:45 PM science upper limit by February 2023. A later crossing time means systematically higher solar zenith angles at observation time, which can bias MODIS cloud optical property retrievals (τ, re) and consequently any derived Nd (Twedt et al., 2023). To date, no formal assessment of CERES MODIS retrieval quality

during the drift period has been published. Could the authors clarify why this study period was chosen, or otherwise, put some discussion on whether the drifting observation geometry may introduce systematic biases into the cloud properties?

Response:

We appreciate the reviewer for drawing our attention to this issue, which was not sufficiently considered in the original manuscript. we have revised the study period from July 2002–February 2023 to July, 2002–December, 2020, corresponding to the temporal coverage of the Nd product from Grosvenor et al. (2018). This revision ensures consistency with the adopted Nd dataset while avoiding the free-drift phase of Aqua. Following this adjustment, all analyses were repeated using the revised study period. The main conclusions of the manuscript remain qualitatively unchanged. Accordingly, all related figures, numerical results, and corresponding discussions have been updated throughout the revised manuscript.

Changes in Manuscript:

[Page 6, Line 117-118 (in the "Track Changes" version)]

Table 1: Overview of datasets used in this study.

Parameter	Data Source	Spatial Resolution	Temporal Resolution	Data Range
Cloud Effective Radius Cloud Optical Thickness Cloud-top Temperature Cloud-top Pressure Liquid Cloud Area Fraction Liquid Water Path	CERES–MODIS V04 SSF1deg (Aqua, daytime)	1° × 1°	daily	Jul 2002 – Feb 2020
Cloud droplet number concentration	Gryspeerdt et al. (2022)	1° × 1°	daily	Jul 2002 – Feb 2020
Total aerosol extinction AOT (550 nm) Total aerosol Ångström parameter (470–870 nm)	MERRA-2	0.5° × 0.625°	daily	Jul 2002 – Feb 2020
Specific Humidity Temperature horizontal wind components mean sea level pressure	ERA5	0.25° × 0.25°	daily	Jul 2002 – Feb 2020
Precipitation	IMERG V07 Final	0.1° × 0.1°	30 min	Jul 2002 – Feb 2020

Sea Surface Temperature	NOAA OI SST V2	1° × 1°	monthly	Jul 2002 – Feb 2020	

Added reference:

Gryspeerdt, E., McCoy, D. T., Crosbie, E., Moore, R. H., Nott, G. J., Painemal, D., Small-Griswold, J., Sorooshian, A., and Ziemba, L.: The impact of sampling strategy on the cloud droplet number concentration estimated from satellite data, Atmospheric Measurement Techniques, 15, 3875–3892, https://doi.org/10.5194/amt-15-3875-2022, 2022.

[Page 13-14, Line 264-265 (in the "Track Changes" version)]

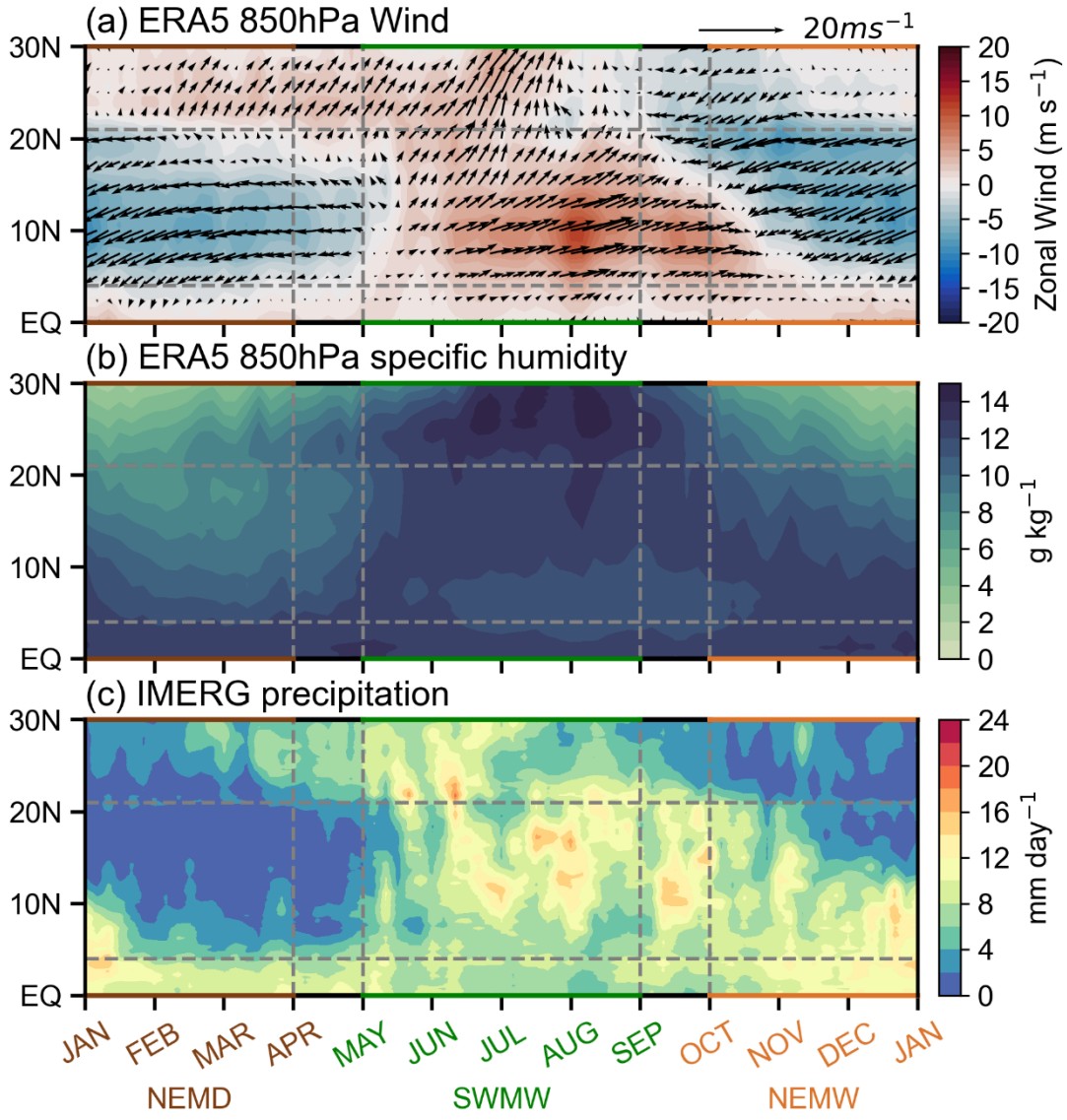

Figure 3: Time–latitude distribution of the (a) ERA5 climatological pentad mean 850 hPa zonal wind (Jul 2002–Feb 2020) and (b) ERA5 pentad mean 850 hPa specific humidity (Jul 2002–Feb 2020) and (c) IMERG

pentad mean precipitation (Jul 2002–Feb 2020). The data are averaged over the longitude bands between 110E and 120E across the SCS. The arrows in (a) indicates 850hPa horizontal winds.

[Page 15-16, Line 264-265 (in the "Track Changes" version)]

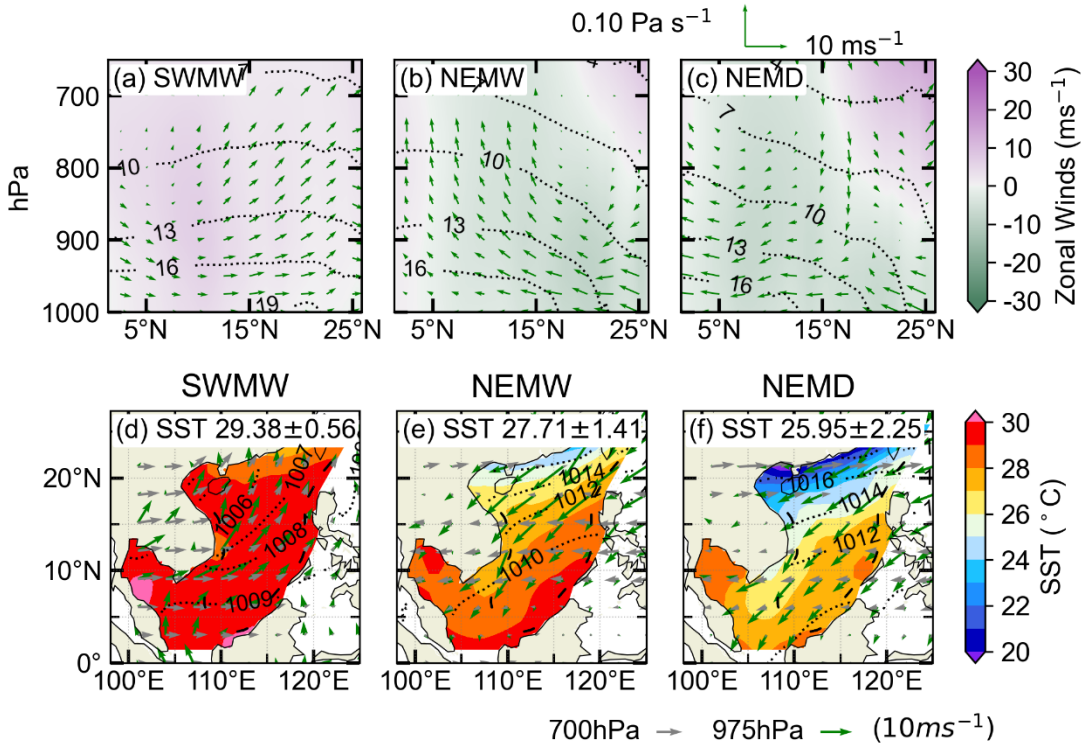

Fig. 4. Zonally averaged cross section of the atmospheric circulation from ERA5 (Jul 2002–Feb 2020) for the domain bounded between 110°E and 120°E during (a) the southwest monsoon wet period, (b) the northeast monsoon wet period, and (c) the northeast monsoon dry period. Meridional and pressure velocity are denoted by arrows (↑ indicates upward motion), whereas colors indicate the zonal wind component. Black contour is specific humidity. Panels (d–f) show the corresponding overview of meteorological conditions and SST over the SCS region. Color shades represent SST from OISST (Jul 2002–Feb 2020), black contour is sea level pressure from ERA5 (Jul 2002–Feb 2020), and arrows are near-surface wind speed at 975 hPa (green) and that at 700 hPa (gray) from ERA5 (Jul 2002–Feb 2020).

[Page 17, Line 308-310 (in the "Track Changes" version)]

Figures 4d–f show that the area-averaged SST over the SCS is highest during the SWMW period (29.38 ± 0.56 °C), lower during the NEMW period (27.71 ± 1.41 °C), and lowest during the NEMD period (25.95 ± 2.25 °C), with variations consistent with those of specific humidity.

[Page 17, Line 320-324 (in the "Track Changes" version)]

The area-averaged aerosol values over the SCS exhibit clear differences among the three periods (Fig. 5). The lowest values occur during the SWMW period, with AOD = 0.17 ± 0.04 and AI = 0.16 ± 0.06. Higher values are observed during the NEMW period, with AOD = 0.23 ± 0.08 and AI = 0.20 ± 0.13, whereas the NEMD period shows the highest values, with AOD = 0.27 ± 0.14 and AI = 0.30 ± 0.23, indicating different aerosol sources. Significant differences in aerosol distribution are also observed between the southwest and northeast periods.

[Page 18, Line 333-337 (in the "Track Changes" version)]

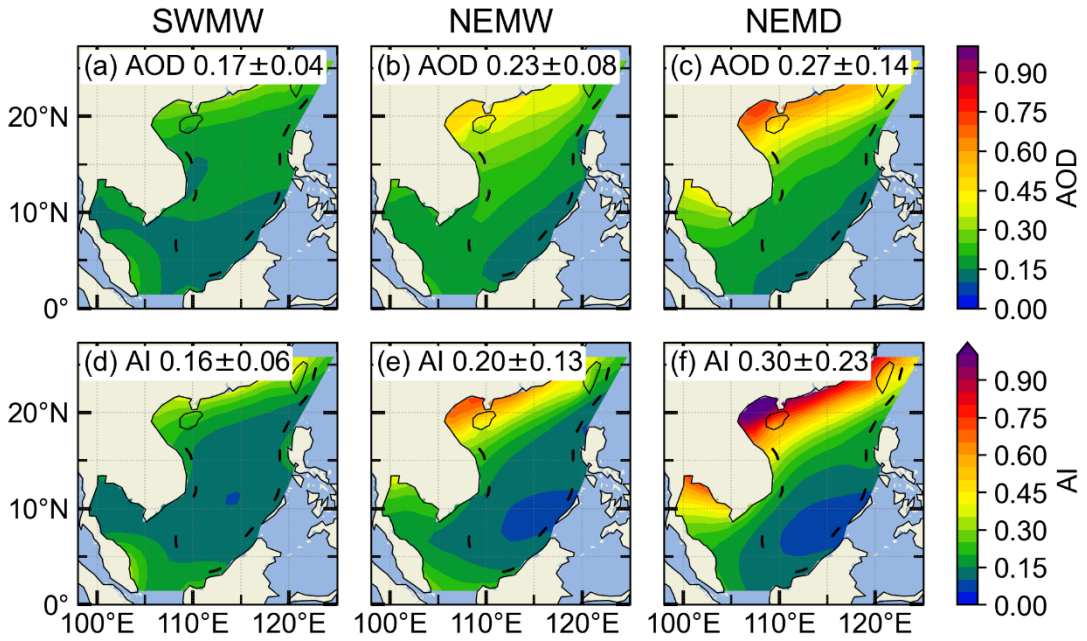

Figure 5: Spatial distributions of MERRA-2 AOD (Jul 2002–Feb 2020) over the South China Sea, averaged over different periods: (a) the southwest monsoon wet period, (b) the northeast monsoon wet period, and (c) the northeast monsoon dry period. (d–f) Corresponding AI (Jul 2002–Feb 2020) averaged over the same periods.

[Page 18, Line 342-343 (in the "Track Changes" version)]

During the SWMW period, the area-averaged warm-cloud fraction over the SCS is the lowest (44.95 ± 16.51 %), whereas comparable higher values are observed during the NEMW (77.21 ± 13.23 %) and NEMD (80.27 ± 11.68 %) periods.

[Page 19-20, Line 350-355 (in the "Track Changes" version)]

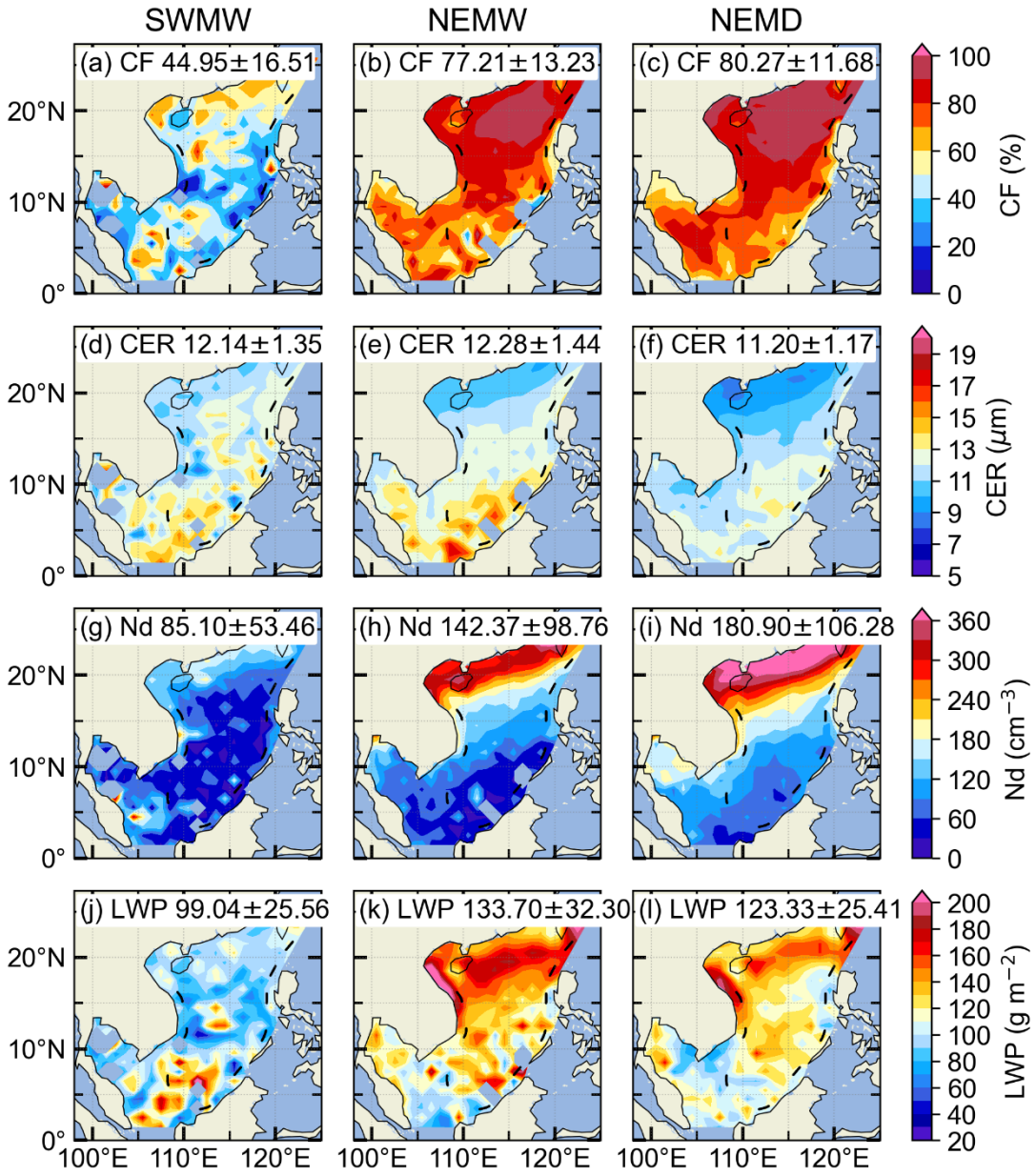

Figure 6: Spatial distributions of warm-cloud (a–c) cloud fraction, (d–f) cloud droplet effective radius, (g–i) cloud droplet number concentration, and (j–l) liquid water path over the South China Sea during the southwest monsoon (first column), the northeast monsoon wet period (second column), and the northeast monsoon dry period (third column).

[Page 20, Line 356-358 (in the "Track Changes" version)]

The area-averaged warm-cloud droplet effective radius over the SCS is similar across the three monsoon periods, with values of 12.14 ± 1.35 μm during the SWMW period,

12.28 ± 1.54 μm during the NEMW period, and 11.20 ± 1.17 μm during the NEMD period (Figs. 6d–f).

[Page 21, Line 363-365 (in the "Track Changes" version)]

The area-averaged warm-cloud droplet number concentration over the SCS exhibits distinct differences among the three periods. The lowest mean value occurs during the SWMW period (85.10 ± 53.46 cm^{-3}), followed by a higher value during the NEMW period (142.37 ± 98.76 cm^{-3}), and the highest value during the NEMD period (180.90 ± 106.28 cm^{-3}) (Figs. 6g–i).

[Page 21, Line 372-374 (in the "Track Changes" version)]

The area-averaged warm-cloud LWP over the SCS is lowest during the SWMW period (99.04 ± 25.56 g m^{-2}), highest during the NEMW period (133.70 ± 32.30 g m^{-2}), and intermediate during the NEMD period (123.21 ± 25.41 g m^{-2}) (Figs. 6j–l).

[Page 23, Line 413-420 (in the "Track Changes" version)]

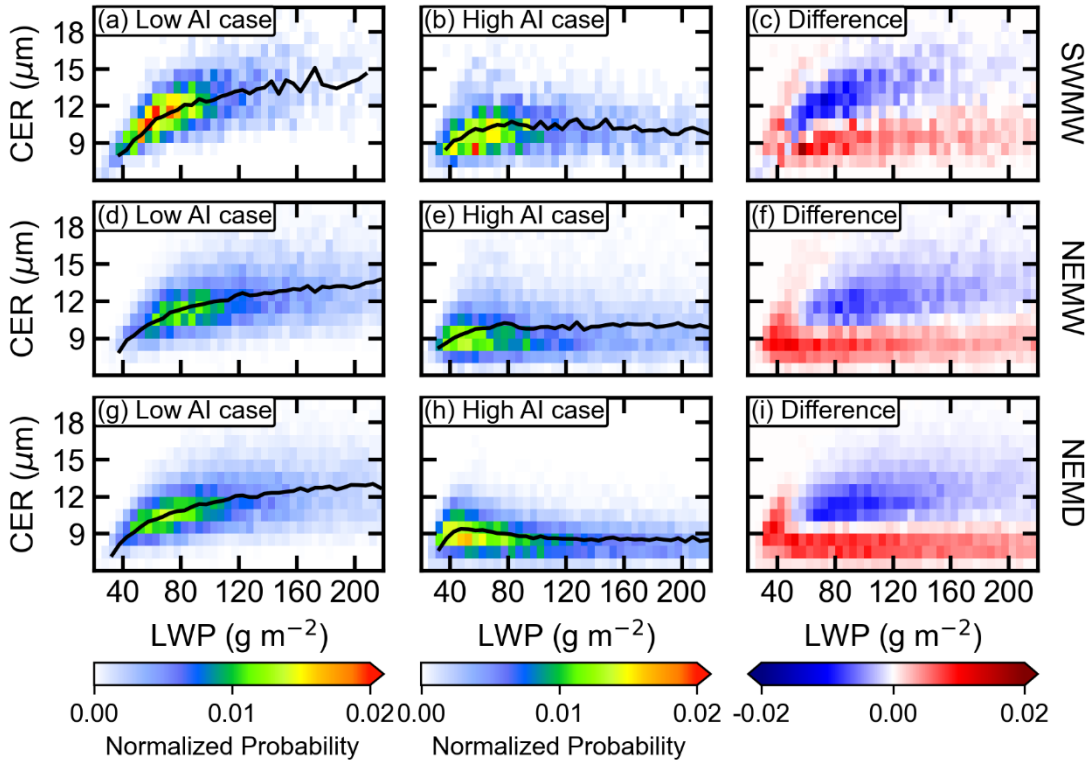

Figure 7: Joint probability distributions of liquid water path (LWP) and cloud droplet effective radius (CER) for warm clouds over the South China Sea during the three periods. The first, second, and third rows correspond to the southwest monsoon, the northeast monsoon wet period, and the northeast monsoon dry period, respectively. The first and second columns represent clean and polluted conditions, respectively. The

black lines denote the mean CER values within each LWP interval. The third column shows the differences in probability density between polluted and clean conditions.

Comment #3:

Satellite Nd derived:

A systematic concern arises from the derivation of cloud droplet number concentration (N_d) using Eq. (3), which is applied to 1° gridded mean cloud properties (τ, re) from the CERES–MODIS SSF product. The N_d formula is a strongly nonlinear function of its inputs, scaling as $\tau^{1/2} \cdot re^{-5/2}$. Applying this formula to grid-box-averaged τ and re, rather than to individual pixel level retrievals, introduces a systematic bias through Jensen's inequality: because $re^{-5/2}$ is a convex function, the mean of $re^{-5/2}$ over a population of pixels is always greater than the function evaluated at the mean re. The practical consequence is that N_d computed from pre-averaged cloud properties will differ systematically from the true grid-box-mean N_d, which should be obtained by first computing N_d at the native MODIS pixel resolution (~1 km) and then spatially averaging.

Moreover, the $re^{-5/2}$ dependence makes this bias particularly severe, because even modest sub-grid variability in re is strongly amplified in the resulting N_d. A 1° × 1° ocean grid box may contain on the order of 10^4 MODIS pixels spanning a wide range of cloud optical thickness and droplet size, including mixtures of polluted and clean clouds, thin and thick clouds, and in some cases liquid-phase and ice-phase pixels. Computing N_d from the grid-box mean of such a heterogeneous population is physically inconsistent with the adiabatic cloud assumption that underlies Eq. (3), which is intended to apply to individual, reasonably homogeneous cloud columns. The South China Sea also presents a challenging environment for satellite N_d retrieval, given the prevalence of broken cumulus and congestus clouds where the adiabatic assumption is less reliable than in stratocumulus-dominated regions.

Furthermore, using the 1° gridded product to derive N_d may forfeits the ability to apply pixel-level quality control filters that are essential for reliable N_d estimation.

Grosvenor et al. (2018) demonstrated that filtering at the pixel level to remove retrievals affected by high solar zenith angles, broken cloud contamination, optically thin clouds ($\tau < 3$), and anomalously large re (indicative of precipitation or multi-layer cloud contamination) is necessary to obtain robust N_d estimates. These filters cannot be meaningfully applied after spatial averaging has already occurred.

The satellite remote sensing community has recognized this issue, and established N_d datasets are constructed by computing N_d at the pixel level before aggregation to coarser grids. I therefore recommend that the authors replace their self-derived N_d with a community-standard product. One option is to compute N_d from the MODIS Level-2 (MYD06/MOD06) pixel-level τ and re retrievals (preferably the 3.7 μm channel) with appropriate quality screening applied at the pixel level, following the recommendations of Grosvenor et al. (2018), and then aggregate the pixel-level N_d to 1° × 1° with caution regarding sampling and filtering choices. Alternatively, the authors could consider the gridded dataset of Gryspeerdt et al. (2022): https://catalogue.ceda.ac.uk/uuid/864a46cc65054008857ee5bb772a2a2b/, which provides 1° × 1° daily N_d computed from pixel-level MODIS Collection 6.1 retrievals (from Aqua and Terra) with multiple validated sampling strategies covering the period 2000–2020, and is well suited for studies of aerosol–cloud interactions of this nature.

Therefore, until the N_d calculation and methodology used in this study is evaluated against aircraft in situ measurements over the South China Sea, I would not put much confidence in the ACI_N relationships derived here. I encourage the authors to either conduct a thorough evaluation of their N_d product against available in situ benchmarks, or to adopt a peer-reviewed and widely recognized MODIS N_d retrieval that has already been validated by the satellite remote sensing community.

Response:

We appreciate the reviewer for raising this important concern regarding the derivation of satellite-based N_d. We agree with the reviewer that deriving N_d directly from 1° × 1° gridded mean cloud properties will introduce systematic biases due to the nonlinear dependence of N_d on cloud optical properties and the inability to apply appropriate pixel-level quality control. In response, we have replaced our originally

self-derived N_d product with the community-standard gridded N_d dataset provided by Edward Gryspeerdt et al. (2022). Following this revision, all analyses were repeated using the updated N_d dataset. Accordingly, all related figures, numerical results, analyses, and corresponding discussions have been revised throughout the manuscript. And the main conclusions remain qualitatively unchanged.

Changes in Manuscript:

[Page 8, Line 165-175 (in the "Track Changes" version)]

N_d used in this study is obtained from the community-standard gridded dataset of Gryspeerdt et al. (2022), which provides 1° × 1° Level-3 N_d products derived from pixel-level MODIS Collection 6.1 retrievals. In this dataset, N_d is first estimated at the native MODIS pixel scale using retrieved cloud optical thickness and cloud effective radius, and then aggregated to a common grid using established sampling strategies to ensure robustness and consistency. The N_d retrievals are based on the adiabatic cloud assumption and are subject to strict quality control procedures, including screening for optically thin clouds, large solar zenith angle and viewing zenith angle conditions, sub-pixel heterogeneity, and potential retrieval contamination. Only single-layer liquid cloud scenes are retained. This dataset has been evaluated against observations and is widely used in aerosol–cloud interaction studies (e.g., Jia et al., 2024; Wall et al., 2023). In this study, we use the N_d_G18_37 product from this community-standard dataset.

[Page 40, Line 725-728 (in the "Track Changes" version)]

Furthermore, the Nd retrieval assumes a constant sub-adiabatic factor (fad = 0.8), which may introduce a systematic offset in Nd estimation (Gryspeerdt et al., 2022). Such an assumption may vary in validity under different meteorological conditions and could potentially introduce seasonal biases, thereby affecting the magnitude of the derived ACI and the inter-period ACI gradient.

Added reference:

Gryspeerdt, E., McCoy, D. T., Crosbie, E., Moore, R. H., Nott, G. J., Painemal, D., Small-Griswold, J., Sorooshian, A., and Ziemba, L.: The impact of sampling strategy on the cloud droplet number concentration estimated from satellite data, Atmospheric

Measurement Techniques, 15, 3875–3892, https://doi.org/10.5194/amt-15-3875-2022, 2022.

Wall, C. J., Storelvmo, T., and Possner, A.: Global observations of aerosol indirect effects from marine liquid clouds, Atmospheric Chemistry and Physics, 23, 13125–13141, https://doi.org/10.5194/acp-23-13125-2023, 2023.

Jia, H., Hasekamp, O., and Quaas, J.: Revisiting Aerosol–Cloud Interactions From Weekly Cycles, Geophysical Research Letters, 51, https://doi.org/10.1029/2024gl108266, 2024.

Comment #4:

Cloud regime confounding across monsoon periods

Section 2.6 (lines 200–213) mentions that all liquid-phase warm clouds with CTT > 273 K, CTP between 650 and 950 hPa, $\tau > 5$, and non-raining conditions are chosen. But it appear that no separation by cloud morphological type is applied. The CTP range of 650–950 hPa is fairly broad, encompassing both shallow marine stratocumulus (typically CTP ~ 850–950 hPa) and deeper trade cumulus or congestus (CTP approaching 650 hPa). As a result, the ACI analysis pools fundamentally different cloud populations together within each monsoon period.

This is consequential because the cloud populations differ substantially between periods. During the SWMW, the warm-cloud fraction is only ~40 % (Fig. 6a), indicating that the warm liquid clouds sampled are a small subset of a convectively active cloud field dominated by deep systems. During NEMD, the warm-cloud fraction reaches ~77 % (Fig. 6c), and the subsidence-dominated environment favors extensive shallow stratiform clouds.

Comparing ACI_r (or ACI_{Nd}) across these periods, even after controlling for LWP, very likely not account for the fact that the underlying cloud dynamical context differs drastically: updraft velocities, entrainment rates, boundary layer depths, and cloud lifetimes are all regime-dependent. For instance, a shallow stratocumulus deck under strong subsidence (NEMD) responds to aerosol perturbations may very differently from isolated trade cumuli embedded in a convectively active boundary layer (SWMW), even at the same LWP.

These differences also affect the satellite retrieval interpretation. The 3.7 μm channel re retrieval is weighted toward cloud top, but the vertical penetration depth depends on cloud optical depth and the vertical profile of droplet size (Platnick, 2000; Grosvenor et al., 2018). For vertically more uniform stratocumulus, the retrieved re approximates the near-cloud-top value reasonably well. However, for cumulus clouds with strong vertical gradients in droplet size and sub-adiabatic profiles due to lateral entrainment, the retrieved re is less representative of the actual cloud-top microphysics. Hence, the CER–AI regression slope (ACIr) may carry different physical meanings across the periods, complicating a direct quantitative comparison.

I suggest that the authors consider separating the analysis by cloud type, or at minimum by CTP sub-ranges that isolate shallow stratiform clouds (e.g., CTP > 800 hPa, corresponding to cloud tops below ~2 km) from deeper cumulus-type clouds. Alternatively, the use of a cloud-regime classification based on joint histograms of τ and CTP (following the ISCCP convention) would enable a more controlled comparison across the three monsoon periods, confining the ACI analysis to a consistent cloud morphological type (e.g., stratocumulus). I would leave that for the authors' consideration.

Response:

We thank the reviewer for pointing this out. Following the suggestion, we further classified the warm cloud population according to cloud-top pressure (CTP) into two distinct cloud regimes: shallow marine stratocumulus (CTP = 800–950 hPa) and deeper cumulus (CTP = 650–800 hPa).

Using the updated Nd dataset from Gryspeerdt et al. (2022), we recalculated both ACI_r and ACI_{Nd} for these two cloud regimes separately. The results show that for shallow marine stratocumulus clouds, both ACI_r and ACI_{Nd} are broadly comparable across the three monsoon periods, with little systematic variation. This suggests that although the large-scale environmental statistics differ substantially among the three monsoon periods, the local thermodynamic conditions favorable for shallow stratocumulus formation may remain relatively similar across periods. Such cloud-favorable environments may not be fully resolved by the period-mean large-scale

statistics presented in this study, which could explain the broadly consistent ACI behavior of shallow marine stratocumulus across the three periods.

In contrast, the deeper cumulus clouds exhibit a clear enhancement in both ACI_r and ACI_{Nd}, with the strongest signals occurring during the Northeast Monsoon Dry period, while weaker values are observed during the Southwest Monsoon Wet and Northeast Monsoon Wet periods, consistent with the overall pattern reported in the original manuscript.

Based on this revised analysis, we have revised the subsequent discussion to focus on the deeper cumulus cloud regime, where the period-to-period differences are clearer and appear to be closely associated with variations in the monsoon environmental conditions. The subsequent analysis further confirms that these differences are consistent with the conclusions of the original manuscript and are primarily modulated by specific humidity and lower-tropospheric stability. The corresponding figures, results, and discussions have been revised accordingly throughout the manuscript.

Changes in Manuscript:

[Page 24-29, Line 421-510 (in the "Track Changes" version)]

As shown in Fig. 6, the warm-cloud fraction during the Southwest Monsoon Wet period is approximately 45%, while it increases to about 77% during the Northeast Monsoon Wet period and further to about 80% during the Northeast Monsoon Dry period. This substantial difference suggests that the warm-cloud populations sampled during different monsoon periods are fundamentally distinct and likely reflect different cloud dynamical regimes. To better distinguish cloud morphological types within each monsoon period and reduce potential regime-mixing effects, we further classified warm clouds over the SCS according to CTP. Specifically, warm clouds were separated into shallow stratocumulus (CTP: 800–950 hPa) and deeper cumulus (CTP: 650–800 hPa) clouds. The ACI index were then quantified separately for these two cloud regimes.

According to the assumption of the Twomey effect (Twomey, 1977), an essential prerequisite for investigating the aerosol indirect effect based on the CER–AI relationship is to keep the LWP constant. Since CER is a function of both LWP and AI, and generally increases with LWP, variations in LWP associated with changes in

aerosols can in turn modulate the CER–AI relationship. Therefore, when applying the CER–AI relationship to analyse the first aerosol indirect effect, it is essential to constrain LWP to ensure its constancy. To satisfy this requirement while maintaining sufficient sample sizes, LWP was binned at 10 g m^{-2} intervals, within which ACI_r was examined separately for shallow stratocumulus (Fig. 8a-b) and deeper cumulus clouds (Fig. 8e-f) during the three periods. The results show that for both shallow stratocumulus and deeper cumulus clouds, under both all warm-cloud conditions and non-raining warm-cloud conditions, ACI_r is generally weak when LWP < 50 g m^{-2}, and even exhibit the anti-Twomey effect (i.e., an increase in CER with increasing aerosol loading). Clouds in this LWP regime are typically very thin or broken, as well as post-precipitation remnants (McComiskey et al., 2009). A similar phenomenon is observed over the northern Indian Ocean, which may be attributed to the intense competition for available water vapor under high aerosol concentrations, combined with the entrainment of dry air at cloud tops (Jose et al., 2020). When LWP > 50 g m^{-2}, the ACI for all cloud regimes across the three periods are consistent with the Twomey effect. An exception occurs in Fig. 8b and Fig. 8d, where the ACI at LWP = 120 g m^{-2} during the southwest monsoon is negative. however, this result is not statistically robust due to the limited sample size.

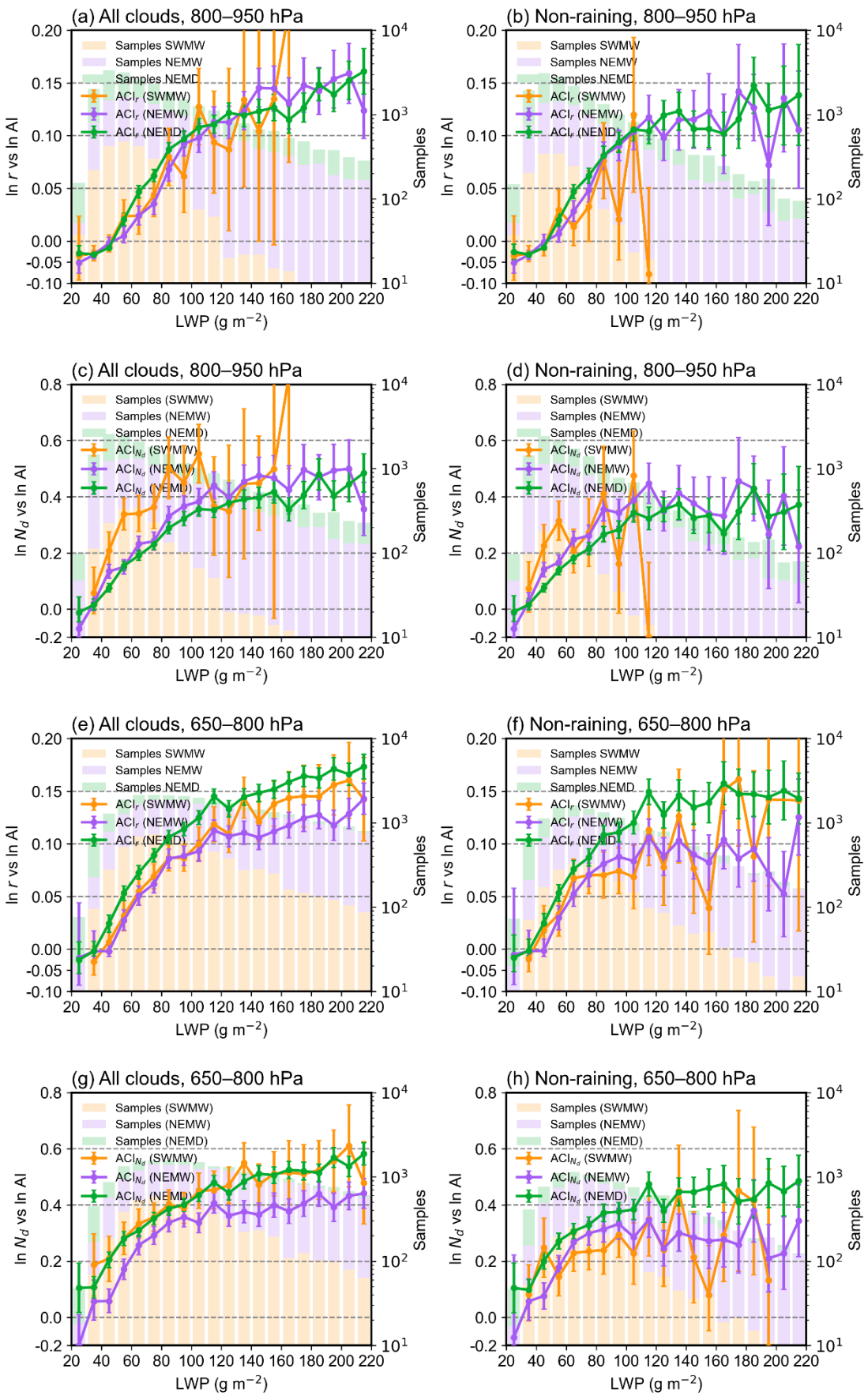
(a) All clouds, 800–950 hPa
(b) Non-raining, 800–950 hPa
(c) All clouds, 800–950 hPa
(d) Non-raining, 800–950 hPa
(e) All clouds, 650–800 hPa
(f) Non-raining, 650–800 hPa
(g) All clouds, 650–800 hPa
(h) Non-raining, 650–800 hPa
Samples SWMW
Samples NEMW
Samples NEMD
ACI$_r$ (SWMW)
ACI$_r$ (NEMW)
ACI$_r$ (NEMD)
ACI$_{N_d}$ (SWMW)
ACI$_{N_d}$ (NEMW)
ACI$_{N_d}$ (NEMD)
ln r vs ln AI
ln N_d vs ln AI
Samples
LWP (g m^{-2})

Figure 8: Linear regression slopes of ln CER versus ln AI and ln N_d versus ln AI for shallow stratocumulus clouds (CTP = 800–950 hPa; a–d) and deeper cumulus clouds (CTP = 650–800 hPa; e–h) during the three periods. The first and second columns represent all cloud and non-raining cloud conditions, respectively. Green, purple, and yellow lines represent the southwest monsoon, northeast monsoon wet period, and northeast monsoon dry period, respectively. Error bars denote the 95 % confidence intervals of the linear regressions. Colored bars, consistent with the line colors, indicate the total number of samples within each LWP bin for the corresponding periods.

Precipitation formation efficiently reduces cloud droplet number concentration and scavenges aerosols from clouds(Gryspeerdt et al., 2015), introducing a sink of that does not reflect the Twomey effect(Jia et al., 2022). Therefore, when analyzing the aerosol first indirect effect in warm clouds, the influence of precipitation should be separated in order to accurately quantify the sensitivity of CER to aerosols. Fig. 8 shows that, for both shallow stratocumulus and deeper cumulus clouds over the SCS, the ACI_r values for all warm cloud are consistently larger than those for non-raining warm-cloud across all three periods when LWP exceeds approximately 80 g m^{-2}. This indicates that the inclusion of raining samples amplifies ACI_r, a phenomenon also identified in the AI/AOD–N_d relationship by Jia et al. (2022) and Painemal et al. (2020). But this amplification is just an artifact governed by the joint impacts of the suppression of precipitation by aerosols and the aerosol removal by precipitation (Jia et al., 2022). Therefore, after removing precipitating clouds from all warm-cloud samples, the ACI_r obtained from non-raining warm clouds provides a more realistic representation.

Fig. 8b. shows that, under non-raining warm-cloud conditions with LWP > 50 g m^{-2}, the period-to-period variations in ACI_r differ between shallow stratocumulus and deeper cumulus clouds over the SCS. For shallow stratocumulus ACI_r values are broadly comparable across the three periods, with no significant differences (Fig. 8b). In contrast, deeper cumulus clouds exhibit clear differences among the three periods (Fig. 8f), with ACI_r generally strongest during the NEMD period, while the NEMW and SWMW periods show comparatively weaker values, with the NEMW period exceeding the SWMW period in some LWP bins. For LWP > 140 g m^{-2}, the ACI_r during the southwest monsoon exhibits large fluctuations due to the limited number of samples, even exceeding that of the northeast monsoon. The analysis in Section 3.2 reveals

substantial differences in atmospheric conditions over the SCS among the three periods. During the SWMW period, atmospheric moisture and sea surface temperatures reach their highest levels, and upward motion dominates over the region, while aerosol concentrations remain relatively low. During the NEMW period, moisture and sea surface temperatures are still relatively high, with upward motion primarily confined to the southern areas near the equator, and aerosol concentrations are elevated due to pollution transported from continental China. In contrast, during the NEMD period, atmospheric moisture and sea surface temperatures are at their lowest, subsidence dominates, and aerosol concentrations reach their maximum. These results suggest that although the large-scale environmental statistics differ substantially among the three monsoon periods, the local thermodynamic conditions favorable for shallow stratocumulus formation may be relatively similar across periods. Such cloud-favorable environments may not be fully resolved by the period-mean large-scale statistics presented here, which could explain the broadly comparable ACI_r values for shallow stratocumulus. In contrast, ACI_r for deeper cumulus clouds over the SCS generally tends to strengthen under drier and more stable monsoon environments, with the strongest signals occurring during the NEMD period, while no consistent ordering is observed between the NEMW and SWMW periods across different LWP bins. Accordingly, the subsequent analysis focuses on the period-to-period differences of deeper cumulus clouds ACI and its relationship with variations in the monsoon environmental background.

In addition to the radius-based ACI_r, we further examined the droplet-number susceptibility (ACI_{Nd}) separately for shallow stratocumulus (Fig. 8c–d) and deeper cumulus clouds (Fig. 8g–h). Consistent with the ACI_r results, ACI_{Nd} for shallow stratocumulus remains broadly comparable across the three monsoon periods, with no significant differences. Deeper cumulus clouds exhibit clear period-to-period variations, with the strongest signals occurring during the NEMD period, while comparatively weaker values are observed during the SWMW and NEMW periods. Such consistency highlights that the observed period-to-period differences in ACI are governed by systematic changes in the underlying meteorological environment rather than by the

choice of ACI metric. Motivated by this consistency, Section 3.5 investigates how variations in moisture and LTS regulate the evolution of deeper cumulus clouds ACI across the three periods.

[Page 39-41, Line 687-737 (in the "Track Changes" version)]

2. A pronounced Twomey effect was consistently identified across all three periods, as indicated by smaller CER and higher Nd with increasing aerosol loading under nearly constant LWP. Quantitative estimates of ACI_r show that the Twomey effect dominates when LWP exceeds 50 g m^{-2}, whereas an apparent "anti-Twomey" behaviour appears in optically thin clouds (LWP < 50 g m^{-2}), likely associated with strong competition for limited water vapor and entrainment-induced drying. Precipitation tends to amplify the ACI by simultaneously suppressing cloud droplet number concentrations and removing aerosols from the atmosphere. After removing raining samples, the ACI derived from non-raining warm clouds provides a more reliable representation of the first aerosol indirect effect, reducing biases caused by precipitation processes. Across the three periods, shallow stratocumulus clouds (CTP: 800–950 hPa) show limited variability in ACI, while deeper cumulus clouds (CTP: 650–800 hPa) exhibit a clear increase from SWMW to NEMW and further to NEMD, reaching a maximum in NEMD.

3. Environmental conditions exert a strong influence on deeper cumulus cloud ACI intensity over the SCS. Water vapor availability may play a critical role in regulating cloud droplet activation and growth. ACI_{Nd} is consistently smaller under moist conditions than under dry conditions across all three periods, indicating that Nd exhibits weaker sensitivity to aerosol perturbations in moist environments compared to dry environments. Thermodynamic stability may also modulate ACI variability. ACI_{Nd} is generally enhanced under stable atmospheric conditions, as stronger LTS may suppress vertical mixing and confine aerosols and moisture within the boundary layer, thereby facilitating aerosol accumulation and potentially promoting CCN activation. Overall, deeper cumulus cloud ACI tends to be more pronounced in dry and stable environments, which are typical of the NEMD, and weakest under moist and convectively active environments during the SWMW. However, these conclusions should be treated with caution, as the present analysis cannot fully disentangle the respective influences of

water vapor, thermodynamic stability, cloud regime, and aerosol type and loading. These factors co-vary systematically with the monsoon phase, which limits attribution of the observed inter-period ACI differences to any single controlling mechanism.

It is worth noting that the use of AI as a CCN proxy may be affected by aerosol hygroscopic swelling, introducing additional uncertainty in the period-to-period variations of deeper cumulus cloud ACI. However, a consistent increasing tendency across the three periods is still observed within all relative humidity bins, indicating that the inter-period differences are not primarily driven by hygroscopic swelling effects, but are more likely controlled by systematic changes in the environmental conditions.

In addition, the coexistence of sea-salt coarse-mode and anthropogenic fine-mode aerosols over the South China Sea introduces uncertainty in using AI as a CCN proxy, particularly due to its limited representation of giant CCN associated with sea salt. This may weaken the diagnosed Twomey effect and introduce additional uncertainty in ACI estimates. Future work will focus on explicitly separating aerosol types to better quantify their respective roles in cloud microphysical processes during different monsoon periods.

Furthermore, the Nd retrieval assumes a constant sub-adiabatic factor ($f_{ad} = 0.8$), which may introduce a systematic offset in Nd estimation (Gryspeerdt et al., 2022). Such an assumption may vary in validity under different meteorological conditions and could potentially introduce seasonal biases, thereby affecting the magnitude of the derived ACI and the inter-period ACI gradient.

Overall, deeper cumulus cloud ACI increases from SW to NEMW and further to NEMD, consistent with co-varying decreases in moisture and increases in atmospheric stability. However, the simultaneous variation of moisture, stability, cloud regime, and aerosol loading across monsoon phases limits the attribution of their individual contributions to the observed inter-period differences. These results highlight that the coupling among aerosols, moisture, and thermodynamic stability exerts fundamental control over marine warm-cloud microphysical processes in tropical monsoon regions. The findings provide important observational evidence for understanding ACI and offer

valuable guidance for improving the representation of ACI in climate and numerical weather prediction models.

Comment #5:

Aerosol hygroscopic swelling artifact

The MERRA-2 total AOD used to construct AI (Eq. 5) is computed at ambient RH, where the extinction coefficients for sulfate, hydrophilic carbonaceous aerosols, and sea salt are explicit functions of relative humidity (Randles et al., 2017). In humid environments, hygroscopic water uptake inflates AOD (and therefore AI) without a corresponding increase in CCN-active particle number. This creates a spurious flattening of the CER–AI and Nd–AI regression slopes under moist conditions, as the AI axis is stretched by swelling rather than by additional CCN. The three monsoon periods differ substantially in humidity (q ~ 12, 11, and 9.5 g/kg for SWMW, NEMW,

and NEMD, respectively), so the progressive strengthening of ACI from SWMW to NEMD (Figs.8b, 8d) could be partly or wholly an artifact of this systematic humidity difference rather than a physical difference in cloud microphysical sensitivity. The same concern applies to the within period humidity stratification (Fig. 10): weaker ACI under moist sub-samples may reflect the swelling artifact rather than the condensational growth and coalescence mechanisms proposed (lines 488–508). This confound has been well documented in the ACI literature (Grandey and Stier, 2010; Quaas et al., 2010).

I would suggest the authors consider acknowledging this potential uncertainty and discussing the extent to which the hygroscopic swelling of the aerosol proxy may limit the interpretation of the humidity-dependent ACI results.

Response:

We sincerely thank the reviewer for raising this important concern regarding the potential observational artifact introduced by aerosol hygroscopic growth. We fully agree that the AOD from MERRA-2, which is calculated under ambient relative humidity conditions, inherently includes aerosol hygroscopic growth effects. This may enhance variations in AI under humid environments and thereby potentially influence the derived ACI regression slopes.

To address this concern, we conducted a systematic sensitivity analysis. Based on our revised cloud-regime analysis (Comment 3), we found that deeper cumulus clouds with cloud-top pressures between 650 and 800 hPa exhibit more pronounced monsoon-dependent differences in ACI, whereas shallow stratocumulus clouds within the 800–950 hPa range show relatively weak ACI differences among the three monsoon periods. Therefore, the subsequent analysis focuses primarily on the deeper cumulus regime (CTP = 650–800 hPa).

On this basis, we further stratified the data from each monsoon period into three relative humidity bins (0–45 %, 45–80 %, and 80–100 %). Under constrained liquid water path (LWP = 50–200 g m^{-2}) and cloud-top pressure (CTP = 650–800 hPa) conditions, ACI was recalculated separately for each subsample. The results show that across all relative humidity bins, ACI consistently exhibits the same enhancement pattern from the SWMW to the NEMW and further to the NEMD period. This indicates that although AI may be affected by hygroscopic growth under humid environments, this effect is insufficient to explain the systematic ACI differences among the three monsoon periods.

Regarding the choice of moisture metric, we prioritize specific humidity (q) rather than relative humidity (RH) in our analysis. This is because relative humidity in the marine boundary layer over the South China Sea is generally close to saturation, with a relatively limited dynamic range, and is strongly modulated by temperature variations, which weakens its ability to represent actual differences in atmospheric moisture content. In contrast, specific humidity provides a more direct measure of absolute atmospheric moisture and is therefore more suitable for characterizing regional moisture background differences.

In addition, because AI in this study is derived from MERRA-2 AOD and the Ångström exponent, and because AOD itself already includes hygroscopic growth effects under ambient RH conditions, it is currently difficult to apply a rigorous “dry-state correction” to the AI proxy. Therefore, we adopted fixed RH stratification to evaluate the sensitivity of ACI to humidity conditions. In future work, we will consider

combining model simulations or dry–wet separated aerosol optical calculations to more systematically quantify the influence of hygroscopic growth on ACI.

We have added relevant discussion to the revised manuscript to explicitly acknowledge this uncertainty and clarify its potential implications for the interpretation of our results.

Changes in Manuscript:

[Page 29, Line 512-534 (in the "Track Changes" version)]

The progressive enhancement of ACI_r and ACI_{Nd} for deeper cumulus clouds from the SWMW to the NEMD period (Fig. 8) may potentially be influenced by the aerosol hygroscopic swelling artifact. The MERRA-2 AOD used to construct AI is calculated under ambient RH, with the extinction coefficients of sulfate, hydrophilic carbonaceous aerosols, and sea salt explicitly parameterized as functions of RH (Randles et al., 2017). Under humid conditions, aerosol hygroscopic growth can increase AOD, and therefore AI, without a corresponding increase in CCN-active particle number. This may artificially flatten the CER–AI and Nd–AI regression slopes, leading to apparently weaker ACI under moister conditions. Given that the SWMW and NEMW periods are characterized by substantially higher moisture levels than the NEMD period, the weaker ACI observed during these moister periods could partly reflect this hygroscopic swelling artifact rather than intrinsic differences in cloud microphysical sensitivity.

To assess whether the observed period-to-period differences are substantially affected by systematic humidity differences, we further stratified the data from each monsoon period into three RH ranges (0–45 %, 45–80 %, and 80–100 %). Under constrained LWP (50–200 g m−2) and cloud-top pressure (650–800 hPa) conditions, ACI_{Nd} was recalculated separately for each subsample. As shown in Table 2, all RH bins consistently exhibit the same enhancement pattern from SWMW to NEMW and further to NEMD. These results suggest that although AI may be affected by hygroscopic swelling under humid environments, this effect is insufficient to explain the systematic ACI differences among the three monsoon periods. Therefore, aerosol hygroscopic swelling is unlikely to be the dominant cause of the observed period-to-

period variability, motivating further examination of the thermodynamic and moisture controls on ACI.

Table 2: ACI_{Nd} ± 95%CI of deeper cumulus clouds under different relative humidity bins during the three periods.

Period	RH<45%	45% ≤ RH < 80%	80% ≤ RH ≤ 100%
SWMW	-0.126 ± 0.291	0.221 ± 0.043	0.278 ± 0.038
NEMW	-0.055 ± 0.194	0.262 ± 0.032	0.312 ± 0.018
NEMD	0.127 ± 0.102	0.371 ± 0.022	0.377 ± 0.012

Added REF:

Randles, C. A., Silva, A. M. da, Buchard, V., Colarco, P. R., Darmenov, A., Govindaraju, R., Smirnov, A., Holben, B., Ferrare, R., Hair, J., Shinozuka, Y., and Flynn, C. J.: The MERRA-2 Aerosol Reanalysis, 1980 Onward. Part I: System Description and Data Assimilation Evaluation, https://doi.org/10.1175/JCLI-D-16-0609.1, 2017.

[Page 40, Line 713-718 (in the "Track Changes" version)]

It is worth noting that the use of AI as a CCN proxy may be affected by aerosol hygroscopic swelling, introducing additional uncertainty in the period-to-period variations of deeper cumulus cloud ACI. However, a consistent increasing tendency across the three periods is still observed within all relative humidity bins, indicating that the inter-period differences are not primarily driven by hygroscopic swelling effects, but are more likely controlled by systematic changes in the environmental conditions.

Comment #6:

ACI-meteorology co-variation

The author finds that ACI strengthens as q decreases and LTS increases from SWMW to NEMD. However, q and LTS are not independent controls. They co-vary tightly with the monsoon phase (Fig. 9 shows this clearly). The within-period stratification (Figs. 10, 11) is a step in the right direction, but the cross-period comparison (which is the headline result) cannot separate the influence of q from LTS from cloud regime from aerosol type and loading, because all of these change simultaneously with the monsoon. The manuscript would benefit from clearly stating

this limitation and being more cautious in attributing the cross-period ACI differences to specific mechanisms.

Response:

We thank the reviewer for pointing this out. We fully agree that specific humidity (q), lower-tropospheric stability (LTS), aerosol conditions, and cloud regimes co-vary systematically with monsoon phase, and therefore cannot be treated as fully independent controls in the cross-period comparison. In the revised manuscript, we have clarified this limitation and toned down the causal interpretation of the cross-period ACI differences. We now emphasize that our results represent a coupled ACI–meteorological co-variation rather than a strictly isolated attribution to individual environmental drivers. Accordingly, we have revised the relevant text throughout the manuscript to avoid over-attribution and to explicitly highlight this limitation in the interpretation of the cross-period results.

Changes in Manuscript:

[Page 39-40, Line 699-712 (in the "Track Changes" version)]

3. Environmental conditions exert a strong influence on deeper cumulus cloud ACI intensity over the SCS. Water vapor availability may play a critical role in regulating cloud droplet activation and growth. ACI_{Nd} is consistently smaller under moist conditions than under dry conditions across all three periods, indicating that Nd exhibits weaker sensitivity to aerosol perturbations in moist environments compared to dry environments. Thermodynamic stability may also modulate ACI variability. ACI_{Nd} is generally enhanced under stable atmospheric conditions, as stronger LTS may suppress vertical mixing and confine aerosols and moisture within the boundary layer, thereby facilitating aerosol accumulation and potentially promoting CCN activation. Overall, deeper cumulus cloud ACI tends to be more pronounced in dry and stable environments, which are typical of the NEMD, and weakest under moist and convectively active environments during the SWMW. However, these conclusions should be treated with caution, as the present analysis cannot fully disentangle the respective influences of water vapor, thermodynamic stability, cloud regime, and aerosol type and loading. These factors co-vary systematically with the monsoon phase, which limits attribution

of the observed inter-period ACI differences to any single controlling mechanism.

[Page 40, Line 729-737 (in the "Track Changes" version)]

Overall, deeper cumulus cloud ACI increases from SW to NEMW and further to NEMD, consistent with co-varying decreases in moisture and increases in atmospheric stability. However, the simultaneous variation of moisture, stability, cloud regime, and aerosol loading across monsoon phases limits the attribution of their individual contributions to the observed inter-period differences. These results highlight that the coupling among aerosols, moisture, and thermodynamic stability exerts fundamental control over marine warm-cloud microphysical processes in tropical monsoon regions. The findings provide important observational evidence for understanding ACI and offer valuable guidance for improving the representation of ACI in climate and numerical weather prediction models.

Comment #7:

Data collocation: Please specify how the different spatial resolution data are collocated.

Response:

In this study, the definitions of the monsoon regimes, as well as the analyses of large-scale atmospheric circulation, aerosol properties, and cloud characteristics, were all performed at their native spatial resolutions. The AOD and AI used in the calculation of ACI, as well as the ERA5 variables used to stratify the analysis according to environmental conditions for AI–CER relationships, were then regridded to a common 1° × 1° grid using bilinear interpolation with the Climate Data Operators (CDO) tool (remapbil). We have now clarified this collocation procedure in the revised Methods section of the manuscript.

Changes in Manuscript:

[Page 5, Line 112-116 (in the "Track Changes" version)]

The definitions of the monsoon regimes and the analyses of large-scale circulation, aerosol, and cloud properties are conducted at their native spatial resolutions. For aerosol–cloud collocation, AOD, AI, and ERA5 meteorological fields used in the

calculation of ACI and environmental stratification are regridded to a common 1° × 1° grid using bilinear interpolation with the Climate Data Operators (CDO, remapbil).

Comment #8:

Here you mentioned AI is used as the aerosol proxy in calculation of ACI, but in the Eq 1) and 2) the CCN is used? Please clarify

Response:

We thank the reviewer for pointing out this inconsistency. We have revised the equations to ensure consistency in the aerosol proxy used throughout the manuscript.

Changes in Manuscript:

[Page 4, Line 74-78 (in the "Track Changes" version)]

$$\mathrm{ACI}_r = -d\ln r / d\ln \alpha \tag{3}$$

$$\mathrm{ACI}_{Nd} = d\ln N_d / d\ln \alpha \tag{4}$$

where r and N_d denote the cloud effective radius and droplet number concentration, respectively, and α is an aerosol proxy (e.g., AOD, AI, or NCCN). In this study, AI is employed as the aerosol proxy in the calculation of ACI.

Comment #9:

Figure 8. If AI is used as CCN proxy, you can directly state Nd (re) vs AI on the Y-axis.

Response:

We thank the reviewer for this helpful suggestion. We have revised Figure 8 accordingly. The corresponding modifications can be found in Comment #3 and the revised Figure 8 in the manuscript.

Responses to Reviewer #2

This study investigates the aerosol-cloud interaction (ACI) susceptibility over the South China Sea across three distinct monsoon periods. While the dataset and the regional focus are valuable, the current methodology and physical interpretations raise several significant concerns. The classification of monsoon periods appears to conflate meteorological effects with aerosol characteristics, and several "findings" seem to align with established knowledge without providing substantial new insights. Furthermore, the physical explanation for ACI sensitivity under high LWP conditions requires more rigorous validation.

Response:

We sincerely thank the reviewer for the careful and constructive review of our manuscript. We agree that several aspects of the original manuscript require further clarification and refinement. We have further clarified the physical meaning of the monsoon classification, emphasizing that it represents a coupled large-scale environmental background state rather than a method for isolating individual causal meteorological factors. We also acknowledge that the Twomey effect is a well-established fundamental physical relationship. The main focus of this study is therefore not to re-establish this known microphysical relationship, but rather to quantify the variability and robustness of aerosol–cloud interaction (ACI) responses under different monsoon-regulated environmental conditions. Regarding the interpretation of ACI behavior under high-LWP conditions, we further clarify that the observed responses are more likely the result of multiple interacting physical processes, rather than being controlled by a single dominant mechanism. We have provided point-by-point responses to your valuable suggestions, aiming to address these issues and enhance the quality of the manuscript.

Comment #1:

The authors categorize the study periods into SWMW, NEMW, and NEMD based on meteorological parameters (humidity and wind at 850 hPa). However, this classification essentially serves as a proxy for cloud types and meteorological regimes.

This method inherently conflates meteorological forcing (stability, moisture) with aerosol loading/type (terrestrial pollution vs. maritime air). It is unclear whether the observed differences in ACI are driven by the monsoon regime itself or simply reflect the underlying aerosol chemical composition and size distribution changes. The authors should perform a sensitivity analysis or a controlled binning (e.g., controlling for LTS and moisture regardless of the monsoon label) to demonstrate if the "monsoon" categorization provides any statistical power beyond standard meteorological grouping

Response:

We thank the reviewer for pointing this issue. The monsoon system represents a natural large-scale circulation background over the South China Sea, consisting of contrasting southwest monsoon and northeast monsoon regimes. In addition, the northeast monsoon period further includes wet and relatively dry sub-stages. Therefore, the monsoon system provides a natural "laboratory" for investigating aerosol–cloud interactions (ACI), enabling the exploration of systematic variability under different coupled environmental states in the real atmosphere.

The "monsoon classification" differs fundamentally from standard meteorological grouping based solely on variables such as lower-tropospheric stability (LTS) or specific humidity (q). Rather than reflecting variations in a single thermodynamic or dynamic factor, the monsoon regimes correspond to three distinct large-scale coupled systems, in which circulation structure, LTS, and moisture, among other thermodynamic and dynamic conditions, evolve coherently as an integrated system. Thus, the monsoon framework should be interpreted as a comprehensive characterization of the regional environmental background state rather than a simple meteorological stratification.

In addition, within each monsoon regime, where both marine background aerosols and continentally transported aerosols are present, ACIr and ACI_{Nd} in deeper clouds consistently exhibit coherent coverability with LTS and moisture conditions. This suggests that even though aerosol composition may differ across monsoon regimes, the ACI response to environmental thermodynamic controls remains highly consistent. Therefore, we infer that the systematic ACI differences observed across the three

monsoon periods are more likely to primarily reflect modulation by the monsoon-driven environmental background itself. And, we acknowledge that differences in aerosol chemical composition and particle size distribution across monsoon regimes may also contribute to the quantitative magnitude of ACI. A more explicit separation and quantification of aerosol compositional effects will therefore be an important focus of future work.

Comment #2:

Figure 7 shows that for a given LWP, higher AI leads to smaller CER, and this behavior is consistent across all three monsoon periods. This is a well established microphysical reality. The authors should clarify what unique insight the monsoon-specific curves provide if the fundamental response is early identical. Aerosol Index (AI) is heavily weighted toward fine-mode articles and often fails to represent coarse-mode sea salt aerosols. In a marine environment like the South China Sea, giant CCN (sea salt) can significantly offset the Twomey effect. The authors must discuss the potential bias introduced by ignoring the contribution of sea salt and coarse particles in their CI calculations.

Response:

We thank the reviewer for this comment. We agree that the negative CER–AI relationship at a given LWP reflects the well-established Twomey effect, which has been extensively documented in previous studies.

The primary purpose of Figure 7 is not to re-establish the existence of the Twomey relationship, but rather to provide a consistent baseline across the three monsoon periods, demonstrating that this fundamental microphysical response remains qualitatively robust under different large-scale meteorological regimes over the South China Sea. On this basis, Figure 7 further serves as a reference framework for the subsequent quantitative analysis, in which we compare the ACI index (ACI_r and ACI_{Nd}) among different monsoon periods under controlled LWP conditions, and investigate whether these differences are associated with variations in the background thermodynamic environment, such as stability and moisture.

And we thank the reviewer for raising this important point regarding the limitation of the aerosol index (AI) in representing coarse-mode sea salt aerosols. We fully acknowledge this potential source of uncertainty.

In this study, AI is used primarily as a proxy for CCN. Compared with AOD, AI incorporates the Ångström exponent, which provides partial information on particle size distribution and therefore reduces the dominance of coarse-mode particles (e.g., sea salt) in the optical signal. Over marine environments such as the South China Sea, this approach helps to mitigate the disproportionate influence of low-number but highly scattering coarse sea-salt particles on AOD, thereby reducing a potential bias in the ACI.

However, we also acknowledge that AI does not fully capture the CCN contribution from coarse-mode marine aerosols. Sea-salt particles, as giant CCN, may modify the droplet size distribution and partially offset the classical Twomey effect, thereby influencing the diagnosed aerosol–cloud relationship. Because AI is less sensitive to coarse-mode particles, their contribution to CCN activity may be underestimated, which could introduce uncertainty in the quantitative magnitude of the retrieved ACI.

We have now explicitly discussed this limitation in the revised manuscript, noting that the neglect of sea-salt aerosol contributions may potentially lead to an underestimation of ACI, and that this issue warrants further investigation in future work.

Changes in Manuscript:

[Page 2, Line 26-27 (in the "Track Changes" version)]

Limitations of AI as a marine Cloud Condensation Nuclei (CCN) proxy and satellite retrieval biases may affect the derived ACI and associated conclusions.

[Page 39-41, Line 699-737 (in the "Track Changes" version)]

3. Environmental conditions exert a strong influence on deeper cumulus cloud ACI intensity over the SCS. Water vapor availability may play a critical role in regulating cloud droplet activation and growth. ACI_{Nd} is consistently smaller under moist conditions than under dry conditions across all three periods, indicating that Nd exhibits weaker sensitivity to aerosol perturbations in moist environments compared to dry environments. Thermodynamic stability may also modulate ACI variability. ACI_{Nd} is

generally enhanced under stable atmospheric conditions, as stronger LTS may suppress vertical mixing and confine aerosols and moisture within the boundary layer, thereby facilitating aerosol accumulation and potentially promoting CCN activation. Overall, deeper cumulus cloud ACI tends to be more pronounced in dry and stable environments, which are typical of the NEMD, and weakest under moist and convectively active environments during the SWMW. However, these conclusions should be treated with caution, as the present analysis cannot fully disentangle the respective influences of water vapor, thermodynamic stability, cloud regime, and aerosol type and loading. These factors co-vary systematically with the monsoon phase, which limits attribution of the observed inter-period ACI differences to any single controlling mechanism.

It is worth noting that the use of AI as a CCN proxy may be affected by aerosol hygroscopic swelling, introducing additional uncertainty in the period-to-period variations of deeper cumulus cloud ACI. However, a consistent increasing tendency across the three periods is still observed within all relative humidity bins, indicating that the inter-period differences are not primarily driven by hygroscopic swelling effects, but are more likely controlled by systematic changes in the environmental conditions.

In addition, the coexistence of sea-salt coarse-mode and anthropogenic fine-mode aerosols over the South China Sea introduces uncertainty in using AI as a CCN proxy, particularly due to its limited representation of giant CCN associated with sea salt. This may weaken the diagnosed Twomey effect and introduce additional uncertainty in ACI estimates. Future work will focus on explicitly separating aerosol types to better quantify their respective roles in cloud microphysical processes during different monsoon periods.

Furthermore, the Nd retrieval assumes a constant sub-adiabatic factor (fad = 0.8), which may introduce a systematic offset in Nd estimation (Gryspeerdt et al., 2022). Such an assumption may vary in validity under different meteorological conditions and could potentially introduce seasonal biases, thereby affecting the magnitude of the derived ACI and the inter-period ACI gradient.

Overall, deeper cumulus cloud ACI increases from SW to NEMW and further to NEMD, consistent with co-varying decreases in moisture and increases in atmospheric

stability. However, the simultaneous variation of moisture, stability, cloud regime, and aerosol loading across monsoon phases limits the attribution of their individual contributions to the observed inter-period differences. These results highlight that the coupling among aerosols, moisture, and thermodynamic stability exerts fundamental control over marine warm-cloud microphysical processes in tropical monsoon regions. The findings provide important observational evidence for understanding ACI and offer valuable guidance for improving the representation of ACI in climate and numerical weather prediction models.

Comment #3:

The authors define "non-precipitating" clouds using an IMERG threshold of < 0.2 mm/h. However, warm clouds with LWP > 200 g/m2 (as seen in Fig 8) are almost certainly undergoing collision-coalescence and likely producing light rain that IMERG may fail to detect. This "hidden" precipitation could lead to a scavenging of aerosols, creating a spurious correlation. The finding that re and Nd sensitivity to AI increases with LWP is counter-intuitive, as one would expect saturation effects or the dominance of collision-coalescence to reduce sensitivity at high LWP. The authors invoke "anti-Twomey" effects, but the physical evidence provided is insufficient. This trend might be a statistical artifact of the LWP-AI co-linearity or the lack of adiabaticity in thick clouds.

Response:

We thank the reviewer for pointing this out. We agree that the IMERG threshold of < 0.2 mm h^{-1} cannot completely exclude all weakly precipitating clouds. In particular, under relatively high-LWP conditions, some warm clouds may already undergo collision–coalescence and produce light drizzle that remains undetected by IMERG.

To address this potential uncertainty, our original manuscript includes a comparison between ACI derived from all warm clouds (including both raining and non-raining samples) and non-raining warm clouds. The results show that ACI for non-raining warm clouds is systematically lower than that for all warm clouds, indicating that the IMERG-based filtering effectively removes a substantial fraction of precipitation-contaminated samples. Although this screening cannot entirely exclude all weak precipitation events, it significantly reduces the influence of precipitation scavenging on the statistical

relationship. Precisely because hidden precipitation may still affect high-LWP clouds, our subsequent analysis focused primarily on the LWP range of 50–200 g m^{-2}, where this potential bias is expected to be partially reduced.

Regarding the reviewer's concern that the increasing sensitivity of Nd and re to AI with increasing LWP appears counterintuitive, we emphasize that this behavior largely arises because our analysis includes the low-LWP regime, where cloud microphysical may response differ substantially from those at moderate and high LWP. Previous studies (e.g., Jose et al., 2020) have shown that under low-LWP conditions (LWP < 75 g m^{-2}) and relatively dry cloud-top environments over the northern Indian Ocean, increasing aerosol loading can lead to statistically significant increases in effective radius, i.e., an anti-Twomey effect. This behavior has been attributed to intensified competition for limited available water vapor under elevated aerosol concentrations, combined with enhanced entrainment of dry air at cloud top.

Therefore, the weak or even negative ACI observed in our low-LWP regime is physically consistent with this mechanism. As LWP increases from approximately 20 to 100 g m^{-2}, cloud liquid water becomes increasingly available, reducing vapor competition constraints and allowing the Twomey response to emerge more clearly, resulting in the observed increase in ACI. Beyond LWP > 100 g m^{-2}, ACI becomes approximately stable rather than continuing to increase.

We clarify that the discussion of the anti-Twomey effect in the original manuscript refers specifically to the very low-LWP regime (LWP < 50 g m^{-2}), representing thin, broken, or post-precipitation remnant clouds, and was not intended to explain the behavior at high LWP.

REF:

Jose, S., Nair, V. S., and Babu, S. S.: Anthropogenic emissions from South Asia reverses the aerosol indirect effect over the northern Indian Ocean, Sci Rep, 10, 18360, https://doi.org/10.1038/s41598-020-74897-x, 2020.

Comment #4:

Figure 9 essentially proves that different meteorological conditions (LTS, moisture) dictate ACI. This conclusion can be reached without the monsoon labels. By "packaging" existing knowledge into monsoon categories, the authors may be obscuring the primary physical drivers rather than revealing new ones. What specific new insight is gained by using the monsoon framework that a simple multi-variate regression with LTS and q would not provide?

Response:

We thank the reviewer for pointing this issue. We agree that the primary contribution of this study is not the proposal of a fundamentally new cloud microphysical mechanism, but rather the identification and quantitative characterization of systematic aerosol–cloud interaction (ACI) differences across distinct monsoon backgrounds over the South China Sea, together with an analysis of the environmental factors responsible for these differences.

The motivation for this study stems from the fact that the South China Sea experiences pronounced seasonal transitions in large-scale circulation, accompanied by systematic changes in atmospheric stability, moisture availability, and cloud structure. We first observed robust aerosol–cloud interaction signals during all three monsoon periods, which led us to ask a more specific question: does ACI exhibit organized and systematic variations under different monsoon-regulated environmental backgrounds within the same region?

Using this framework, we found that for relatively deeper warm cumulus clouds with cloud-top pressures between 650–800 hPa, ACI exhibits a clear progressive enhancement from SWMW to NEMW and further to NEMD, whereas such differences are much weaker for shallower stratiform clouds (800–950 hPa). Further analysis shows that this systematic gradient closely covaries with background lower-tropospheric stability (LTS) and specific humidity (q), indicating that the combined modulation of atmospheric stability and moisture availability may explain the observed ACI differences.

Therefore, the purpose of adopting the monsoon framework is not to replace standard meteorological controls such as LTS and q with categorical labels, but rather to use the naturally occurring monsoon transitions over the South China Sea as a physically meaningful regional-scale environmental classification that organizes these coupled variations. Compared with a simple multivariate regression using LTS and q, the monsoon framework provides an additional physically interpretable regional context by revealing how ACI responds systematically to transitions between large-scale environmental regimes. This allows the results to be interpreted not merely as statistical correlations, but as regionally coherent process-level responses linked to monsoon-driven environmental changes.

Comment #5:

Adiabatic Assumption: The use of a constant adiabatic fraction fad = 0.7 to calculate Nd is problematic. Entrainment-mixing processes vary significantly between the moist SWMW and the drier NEMD. A fixed fad may introduce systematic biases in Nd across seasons, artificially inflating or deflating the ACI indices.

Response:

We thank the reviewer for raising this important point. We agree that the use of a fixed adiabatic fraction may introduce systematic uncertainty.

Following Reviewer 1's comment (Comment# 3), we have replaced the originally calculated Nd with a community-standard gridded dataset provided by Gryspeerdt et al. (2022). Although this retrieval also adopts a fixed fad assumption, its retrieval algorithm employs a more robust sampling strategy and shows good agreement with observations, thereby reducing retrieval uncertainty and improving the reliability of the Nd dataset.

More importantly, our main conclusion does not rely solely on ACI_{Nd}. In the analysis, both ACI_r and ACI_{Nd} exhibit a consistent inter-period gradient, with susceptibility progressively increasing from SWMW to NEMW and then to NEMD. Since ACI_r does not depend on the fixed-fad assumption used in Nd retrieval, this consistency suggests that the fixed fad assumption is unlikely to alter the relative seasonal ranking of ACI.

we acknowledge that the fixed-fad assumption remains a limitation of Nd retrieval. We have added a discussion in the revised manuscript to explicitly state that this assumption may contribute to an offset in the retrieved Nd and thus affect the magnitude of ACI_{Nd}.

Changes in Manuscrip

[Page 40, Line725-728 (in the "Track Changes" version)]

Furthermore, the Nd retrieval assumes a constant sub-adiabatic factor (fad = 0.8), which may introduce a systematic offset in Nd estimation (Gryspeerdt et al., 2022). Such an assumption may vary in validity under different meteorological conditions and could potentially introduce seasonal biases, thereby affecting the magnitude of the derived ACI and the inter-period ACI gradient.

REF:

Gryspeerdt, E., McCoy, D. T., Crosbie, E., Moore, R. H., Nott, G. J., Painemal, D., Small-Griswold, J., Sorooshian, A., and Ziemba, L.: The impact of sampling strategy on the cloud droplet number concentration estimated from satellite data, Atmospheric Measurement Techniques, 15, 3875–3892, https://doi.org/10.5194/amt-15-3875-2022, 2022.

Comment #6:

MERRA-2 aerosol products in the SCS region have known discrepancies, particularly regarding biomass burning plumes and sea salt concentrations. The authors should validate these aerosol fields against AERONET or other independent observations if available.

Response:

We sincerely thank the reviewer for the valuable suggestion regarding the evaluation of MERRA-2 aerosol products in the South China Sea (SCS). In response, we have further validated MERRA-2 aerosol optical depth (AOD) and aerosol index (AI) using AERONET observations from two representative sites: Dongsha Island (20.70°N, 116.73°E) in the northern SCS and Taiping Island (10.38°N, 114.37°E) in the southern SCS. Dongsha Island is a small subtropical coral atoll with minimal local emissions (limited mainly to airport-related activity) but is frequently influenced by

continental outflow. In contrast, Taiping Island is a remote marine site with little continental influence, representing a typical marine background atmosphere.

We compared MERRA-2 AOD and AI against AERONET observations for the full period, as well as during the southwest monsoon wet season, northeast monsoon wet season, and northeast monsoon dry season, as shown in Fig. 1. Overall, MERRA-2 shows reasonable agreement with AERONET at both sites. Differences are observed between the two stations. At Dongsha Island, the correlation coefficients (R^2) between MERRA-2 and AERONET are generally higher than those at Taiping Island (except during the southwest monsoon period). In addition, AI consistently outperforms AOD at Dongsha Island across all seasons, whereas at Taiping Island, AI only shows better performance than AOD during the northeast monsoon dry season.

These differences likely reflect distinct aerosol regimes at the two sites. Dongsha Island is more strongly influenced by continental transport and biomass burning–related fine-mode aerosols, while Taiping Island is dominated by coarse-mode marine aerosols such as sea salt. Therefore, MERRA-2 provides a more robust representation of fine-mode aerosol variability, whereas larger uncertainties remain in simulating coarse-mode marine aerosols. Overall, the AERONET comparison suggests that although MERRA2 exhibits certain biases under different aerosol regimes, particularly under coarse-mode sea salt–dominated conditions, it still captures the regional-scale variability and relative changes of aerosols reasonably well.

Importantly, the primary objective of this study is not to quantitatively evaluate absolute aerosol emissions or chemical composition, but to investigate aerosol–cloud interactions (ACI) and their dependence on large-scale meteorological conditions, such as monsoon regimes and lower-tropospheric stability (LTS). From this perspective, the systematic differences between MERRA-2 and AERONET at individual sites do not affect the main conclusions of this study, which are based on relative variations and statistical relationships rather than absolute aerosol magnitudes.

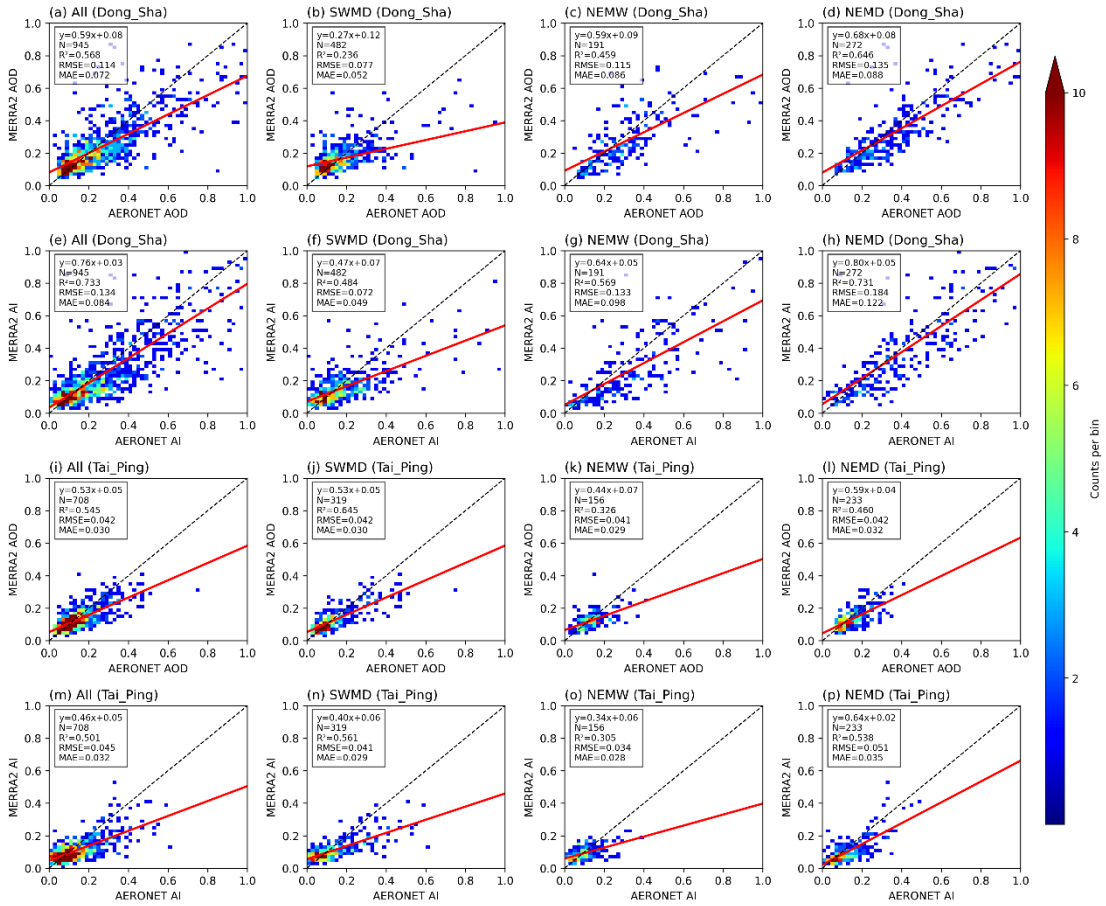

Fig. 1. Evaluation of MERRA-2 aerosol optical depth (AOD) and aerosol index (AI) using AERONET observations. Panels (a–h) show results for Dongsha Island, while panels (i–p) show results for Taiping Island. Columns from left to right represent all periods, southwest monsoon wet season, northeast monsoon wet season, and northeast monsoon dry season, respectively.

Method:

For consistency in the comparison, AERONET AOD at 500 nm was converted to 550 nm using the Ångström power-law relationship:

$$\tau_{550} = \tau_{500}\left(\frac{550}{500}\right)^{-\alpha}$$

where τ500 is the aerosol optical depth at wavelength 500nm, and α is the Ångström exponent (AE) for 440 and 870 nm.

Comment #7:

The manuscript is excessively long and contains redundant descriptions of standard ACI formulas. I suggest streamlining the text to focus on the unique physical mechanisms (if any) that differentiate the monsoon regimes.

Response:

We thank the reviewer for this helpful suggestion. In response, we have substantially revised the manuscript to improve clarity and reduce redundancy.

Specifically, following Reviewer 1's comment (Comment# 1), we have revised the ACI formulation and removed the independently retrieved Nd calculation, replacing it with a mature satellite-based Nd product (Gryspeerdt et al., 2022). This change simplifies the methodological description and reduces potential redundancy in the text.

In addition, we have expanded the discussion of key sources of uncertainty affecting ACI, including the hygroscopic growth of aerosol proxies, the potential impact of neglecting coarse-mode sea-salt aerosol contributions, and the uncertainties associated with the assumption of a fixed sub-adiabatic factor in the Nd retrievals. These factors may introduce additional uncertainties in the quantitative magnitude of the derived ACI.

Again, please to check this revised manuscript version and response files. We hope that the above responses can meet the concerns of the reviewers and the requirements of the journal. Thanks.

Dr. Yong Han (prof.)

ASAG, School of Atmospheric Sciences, SYSU, China

E-mail: hany66@mail.sysu.edu.cn